NASA-CR-73444
WANL PR(TTT)-001

STUDY OF FABRICATION TECHNIQUES FOR SiC SOLAR CELLS

by

R.B. Campbell
and
H.S. Berman

Westinghouse Astronuclear Laboratory

FINAL TECHNICAL REPORT

July, 1970

NATIONAL AERONAUTICS AND SPACE ADMINISTRATION

NASA Ames Research Center
Under Contract NAS 2-5595
Technical Monitor - C.A. Lewis

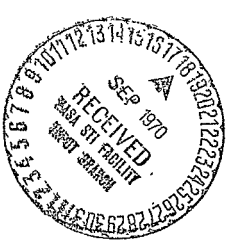

Astronuclear Laboratory
WANL PR(TTT)-001
NASA-CR-73444

STUDY OF FABRICATION TECHNIQUES FOR SiC SOLAR CELLS

by

R. B. Campbell
and
H. S. Berman

FINAL TECHNICAL REPORT

July, 1970

NATIONAL AERONAUTICS AND SPACE ADMINISTRATION
Ames Research Center
Under Contract NAS 2-5595
Technical Monitor - C. A. Lewis

ASTRONUCLEAR LABORATORY
WESTINGHOUSE ELECTRIC CORPORATION

THIS SHEET INTENTIONALLY LEFT BLANK

SUMMARY

Silicon carbide unijunction diodes have been investigated for use as possible solar cells. The devices can be used in this manner, although the overall conversion efficiency of solar energy into electrical energy is much lower than Si diodes. This lower efficiency is due mainly to fewer photons of proper energy available for conversion, reflection losses and poor collection efficiency in the SiC diode. Both grown and diffused junctions were investigated. A graded junction structure with a junction depth of 15 microns was determined to be optimum. Techniques for applying gridded contacts were developed. The single junction cells exhibited maximum power at 250°C although they were operable at reduced efficiency to 400°C and would survive temperatures to 1000°C without damage. The cells operated satisfactorily when connected in series and parallel configurations. Several other cell structures such as the multiple junction and multiple transition were investigated. These structures show a greatly increased efficiency over the single junction cell although further work is needed to develop these structures. Additional work is also required in the growth of larger more perfect cyrstals and the development of an anti-reflection coating.

Symbols

Å - Angstroms

AU - Astronomical unit (mean distance between earth and sun)

α - Absorption coefficient (cm^{-1})

E - Band gap (electron volt)

$h\gamma$ - Energy of photon

THIS PAGE INTENTIONALLY LEFT BLANK

TABLE OF CONTENTS

LIST OF FIGURES

LIST OF FIGURES (CONTINUED)

I. INTRODUCTION

In solar orbital missions, the spacecraft will be subjected to high temperatures and radiation flux. For example, at missions within 0.2 AU of the solar surface, temperatures will exceed 250°C. This temperature would require cooling of standard Si solar cell panels. In this program we are investigating an alternative solution to this problem which is the use of SiC solar cells operable to 400°C.

A solar cell is essentially a semiconductor with a p-n junction arranged so that radiant energy falling on the crystal is converted to electrical energy. This conversion to electrical energy is accomplished by the junction field separation of the electrons and holes produced by the absorbed light.

SiC is a wide band gap semiconductor with a band gap near 2.7 eV at 300°C. It is stable at high temperatures and practically inert to most oxidizing and reducing compounds. Due to its band gap, photons will be absorbed only when their energy is greater than 2.7 eV (or when the wavelength is shorter than 4200 Å). Of the total energy of the solar spectra (at air mass zero), approximately 12 percent is contained in radiation with wavelengths less than 4200 Å [1]. A Si solar cell, on the other hand, can absorb over 60 percent of the solar radiation (roughly from 4000 Å to 11,000 Å) since the band gap of Si is 1.1 eV. Thus, intrinsically a Si solar cell makes more efficient use of the solar spectrum than a SiC device. However, with a mission of 0.2 AU orbit, the intensity of solar radiation would be 25 times as great as at 1.0 AU, therefore even though the SiC cell can use only about 12 percent of this radiation, it will receive (at 0.2AU) nearly six times the energy of a Si cell at 1.0 AU.

This feasibility program to investigate SiC unijunction crystals as solar cells consists of three basic tasks:

Task 1: Calculation of the optimum characteristics that could be expected from the SiC unijunction crystals, and methods needed to approach this optimum characteristic. This study will also include an examination of more complex junction structures and

preparation techniques such as epitaxial films, multiple junction devices (both constant and varying band gaps) and multiple transition cells,

Task 2: A study of techniques needed to fabricate unijunction solar cells along with interconnection methods, and

Task 3: Delivery of twenty-five (25) silicon carbide solar cell structures.

During the program a number of grown junction and diffused junction devices were tested in a rudimentary solar simulator as a function of temperature. This simulator consisted of a 275 watt tungsten sunlamp mounted inside an air cooled chamber. A heated stage sample holder, capable of 400°C operation in an inert gas atmosphere was positioned six inches below the lamp. No absolute measurements were made, but using previously calibrated SiC photodiodes, the intensity was estimated at 55 mw/cm^2 $\pm$ 10 mw/cm^2. It was found that a very graded junction structure was required for operation at 400°C. Such graded junctions can most readily be produced by diffusion.

Using solar spectrum data, it was determined that the optimum junction depth for a SiC solar cell should be near 15 microns. At this depth, the spectral peak would be about 3900 Å. Although most of the shorter wave length radiation ($\lambda <$ 3400 Å) will be lost by absorption and recombination near the surface, the larger flux of longer wave length radiation more than compensates for this loss.

Techniques for making top gridded contacts were developed. Tungsten mesh having a 4 mil line width on 42 mil centers (82% transmission) was used as a grid and can be hard soldered to the cell using AuTa alloy. A conductive, high temperature epoxy was put down in a grid pattern and found to be equally effective.

Interconnection problems were studied to the extent of measuring matched (resistance) and mismatched diodes in series and parallel configuration. No parasitic self-loading or other effects were noted in either case.

A paper study was made of several different solar cell geometries. The most promising (and certainly the one which needs the most further study) is a multiple transistion cell. An increase in solar spectrum utilization of an order of magnitude could be expected from a three level device. The multijunction device was also studied and the utilization factor would increase by a factor of two or three.

During the period of the program, a number of cell structures were fabricated and evaluated. The twenty-five devices having the best properties (highest power output) are delivered with this report.

II. DEVICE DESIGN

Since the SiC unijunction solar cell will absorb only radiation with wavelengths shorter than the band gap energy equivalent (≈ 4200 Å), optimum use must be made of the solar spectrum below 4200 Å. This involves optimum junction placement and a wide depletion width.

Figure 1 shows that the wavelength at which the spectral peak of the device occurs is a function of the junction depth. This information, together with the behavior of the absorption coefficient of SiC as a function of wavelength and temperature, and the solar spectrum as a function of wavelength can provide the optimum junction depth.

Using the analytical expression developed by Choyke and Patrick[2] for SiC:

$$\alpha = A \left[\frac{(h\gamma - Eg + k\Theta)^2}{e^{\Theta/T} - 1} + \frac{(h\gamma - Eg - k\Theta)^2}{1 - e^{-(\Theta/T)}} \right]$$

where:

α	=	absorption coefficient
$h\gamma$	=	photon energy
Eg	=	minimum energy gap
$k\Theta$	=	energy of the phonon (absorbed or emitted)
A	=	material constant depending on electron-phonon interaction

The above was calculated to obtain the absorption coefficient (α) as a function of wavelength and temperature. These results are shown graphically in Figure 2 which is a plot of absorption coefficient versus temperature for selected wavelengths.

This information is shown in different form in Figure 3 which is a plot of the absorption edge of SiC at room temperature and 400°C. As can be seen, there is a significant

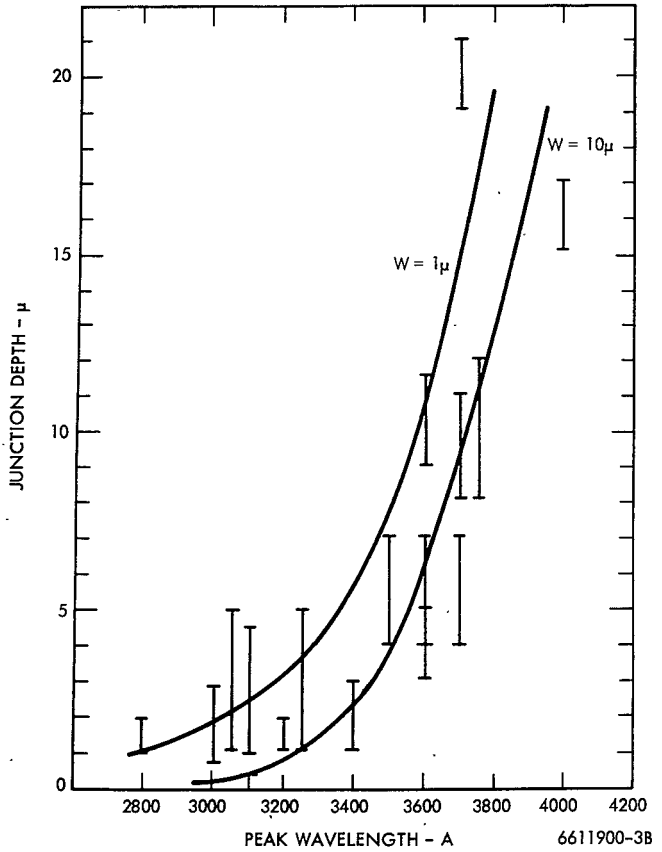

FIGURE 1. Junction Depth vs Peak Wavelength (30°C)

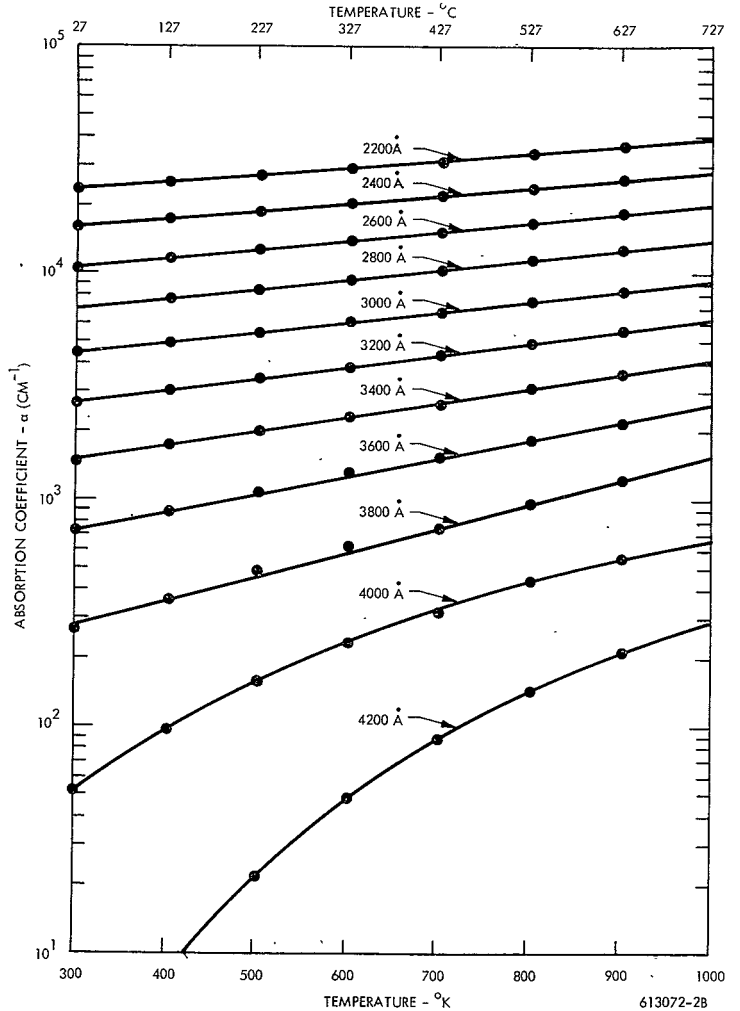

FIGURE 2. Absorption Coefficient as a Function of Wavelength and Temperature for Alpha Silicon Carbide

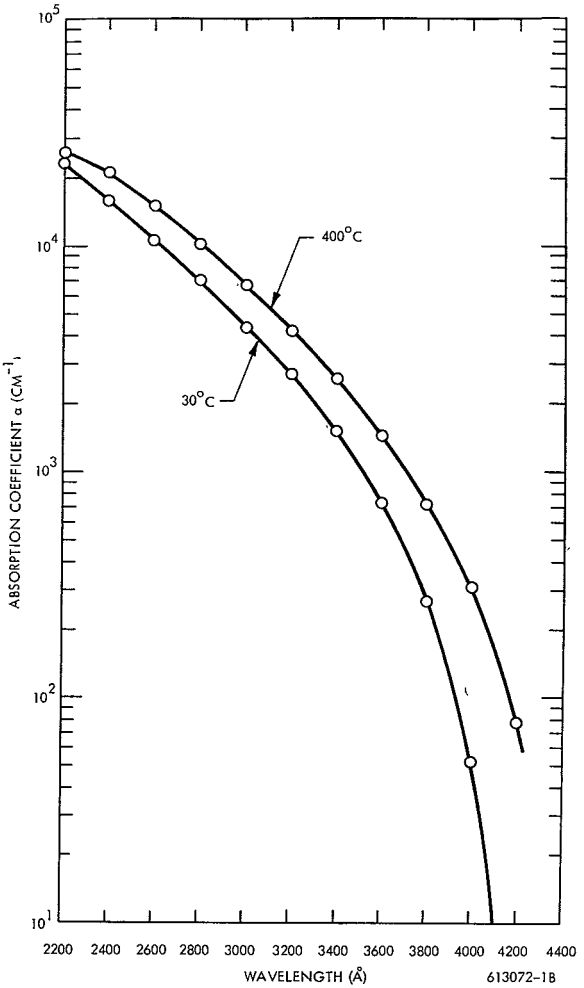

FIGURE 3. Absorption Coefficient vs Wavelength of Incident Light on Alpha Silicon Carbide at 30°C and 400°C.

difference at these temperatures (e.g. at 400°C there is about six times the absorption for 4000 Å light than at 30°C at the same distance into the crystal). Thus the junction optimization procedure should take these factors into account. A cell optimized for high temperature use will be less than optimum at lower temperatures and vice-versa. Utilizing this data, calculations were made for percent light absorbed as a function of distance into the SiC crystal for different wavelengths and temperatures. These calculations are shown graphically in Figure 4.

These data were then combined with solar spectrum data to indicate the junction depth which would permit the most efficient use of sunlight.

Using data of Johnson[1] on the solar energy per unit wavelength at air mass zero, the solar photon flux was calculated. This is presented in tabular form in Table 1 and graphically in Figures 5 and 6.

As can be noted from Figure 6, the number of photons/cm^2/sec in sunlight does not diminish significantly until we get below about 3500 Å. This figure also indicates that the solar cell junction should be deep enough to absorb the majority of the light in the 4400 to 3900 Å region, where there is the greatest number of usable photons. Returning to Figure 4 which is a plot of the absorption of light into alpha silicon carbide as a function of distance from the surface, it appears best to utilize the 4200 to 3900 Å photons with the junction depth centered around fifteen microns. However, some information on the collection width needs to be obtained. The larger the depletion width over which we can collect photon generated electron-hole pairs, the closer to the surface the junction region should be placed.

The limit, of course, occurs if we can collect carriers over a 30 micron or larger depletion layer which would put the junction almost at the surface and enable us to utilize almost all of the sunlight from 3000 to 4200 Å. This is probably not feasible and additionally, the larger the depletion width, the higher is the junction resistance.

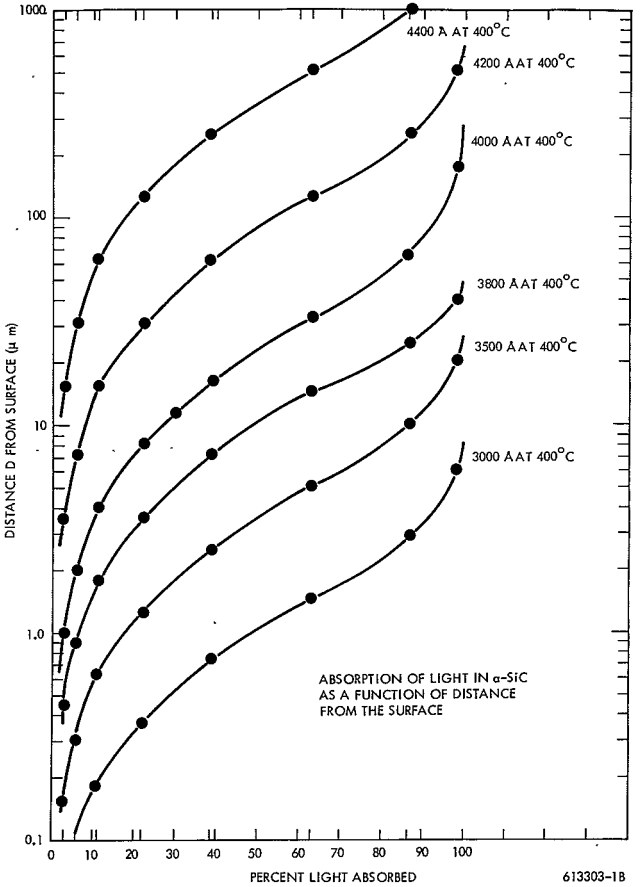

FIGURE 4. Absorption of Light in Alpha SiC as a Function of Distance from the Surface (400°C)

Table 1. Solar Spectra Data – Energy and Photon Flux per Unit Wavelength (Air Mass Zero)

(Å)	eV/Photon	Joules/Photon	Solar Energy (watts/cm^2/μm)	Solar Flux Photons/sec/cm^2
2200	5.64	9.04×10^{-19}	0.0030	3.31×10^{15}
2500	4.96	7.95×10^{-19}	0.0064	8.05×10^{15}
2600	4.77	7.65×10^{-19}	0.013	1.69×10^{16}
2700	4.59	7.36×10^{-19}	0.025	3.39×10^{16}
2800	4.43	7.10×10^{-19}	0.024	3.38×10^{16}
2900	4.27	6.84×10^{-19}	0.052	7.6×10^{16}
3000	4.13	6.62×10^{-19}	0.061	9.21×10^{16}
3100	4.00	6.41×10^{-19}	0.076	1.19×10^{17}
3200	3.87	6.20×10^{-19}	0.085	1.37×10^{17}
3300	3.75	6.01×10^{-19}	0.115	1.91×10^{17}
3400	3.64	5.83×10^{-19}	0.111	1.90×10^{17}
3500	3.54	5.67×10^{-19}	0.118	2.08×10^{17}
3600	3.44	5.51×10^{-19}	0.116	2.11×10^{17}
3700	3.35	5.37×10^{-19}	0.133	2.47×10^{17}
3800	3.26	5.23×10^{-19}	0.123	2.35×10^{17}
3900	3.17	5.08×10^{-19}	0.112	2.20×10^{17}
4000	3.10	4.97×10^{-19}	0.154	3.10×10^{17}
4200	2.95	4.73×10^{-19}	0.192	4.06×10^{17}
4300	2.88	4.62×10^{-19}	0.178	3.85×10^{17}
4400	2.82	4.52×10^{-19}	0.203	4.49×10^{17}
4500	2.75	4.41×10^{-19}	0.220	4.99×10^{17}
5000	2.48	3.98×10^{-19}	0.198	4.97×10^{17}
5500	2.25	3.60×10^{-19}	0.195	5.42×10^{17}
6000	2.06	3.41×10^{-19}	0.181	5.30×10^{17}
6500	.191	3.06×10^{-19}	0.162	5.29×10^{17}
7000	1.77	2.84×10^{-19}	0.144	5.07×10^{17}
7500	1.65	2.64×10^{-19}	0.127	4.81×10^{17}
8000	1.55	2.48×10^{-19}	0.113	4.56×10^{17}
8500	1.46	2.34×10^{-19}	0.1003	4.29×10^{17}
9000	1.37	2.20×10^{-19}	0.0895	4.07×10^{17}

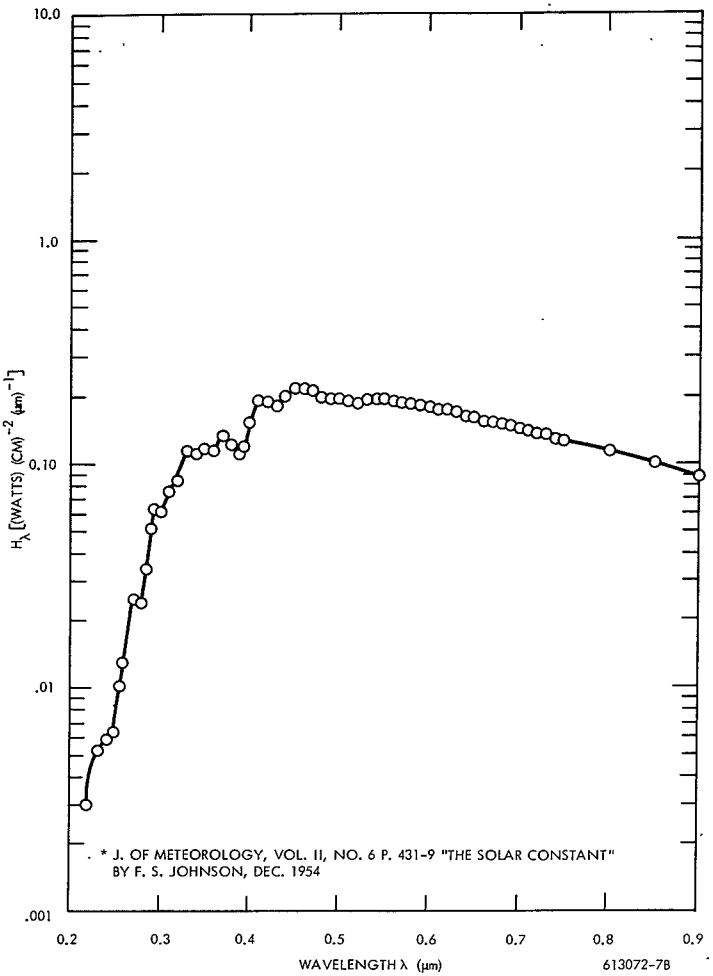

FIGURE 5. Solar Energy versus Wavelength at Air Mass Zero

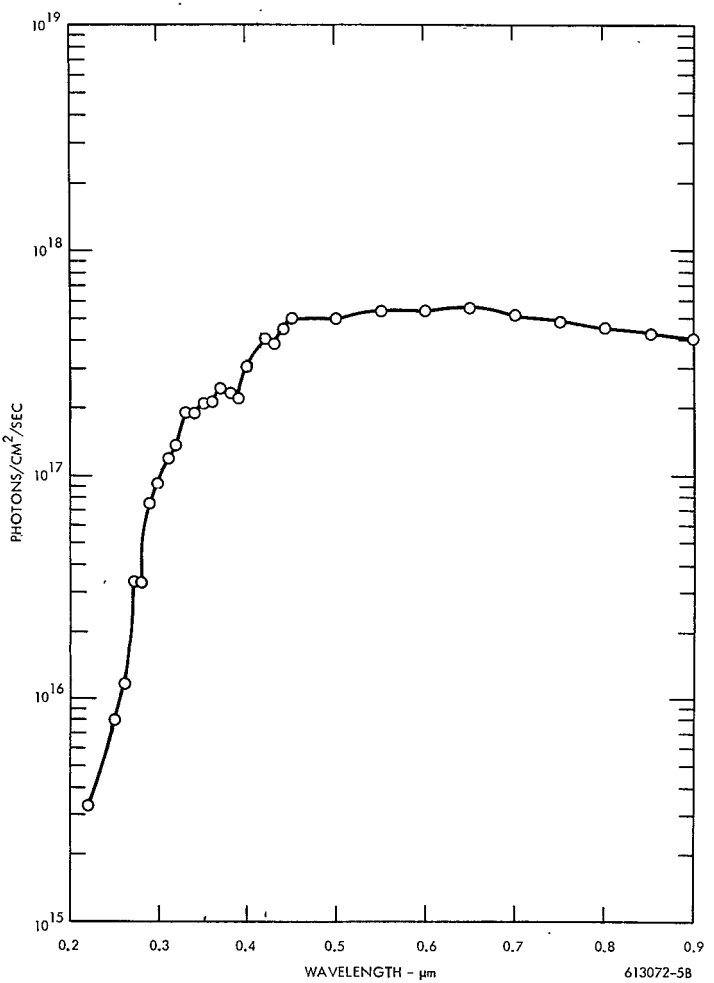

FIGURE 6. Solar Photon Flux versus Wavelength at Air Mass Zero

In summary, the optimum structure for a SiC unijunction solar cell would have a graded junction about 15 microns deep.

III. FABRICATION TECHNIQUES

A. CRYSTAL GROWTH

A study of the growth of SiC crystals was not included in the present program, however for completeness the growth technique will be described.

SiC does not have a melting point and the crystals are normally grown by a vaporization-condensation process near 2500°C. This growth is carried out in a large resistance heated furnace[3],[4] using powdered graphite as a thermal insulator. This large volume furnace and the insulation makes it difficult to remove the various impurities which can dope the SiC. These are mainly nitrogen (an n-type dopant) and aluminum and boron, (p-type dopants).

The crystals are grown inside a thin graphite cylinder surrounded by granular SiC. When the temperature of the growth cavity is raised to near 2500°C, the SiC in the granular charge vaporizes, diffuses through the graphite growth cylinder and nucleates on the inner wall. The grown crystals are usually hexagonal platelets.

In many cases it is desirable to grow a p-n junction in the crystals. This is accomplished by adding an impurity of one type during the initial stage of the growth and of a second type during the latter stages. This leads to a crystal having a bulk conductivity of one type (e.g. p-type) with an n-type surface. The junction structure can be graded within certain limits by varying the amount and time of introduction of the dopants.

The use of these grown junction crystals was studied in the initial stages of the program.

Pure crystals can be grown using an extensive heating and outgassing cycle to remove the metallic impurities and reduce the nitrogen level in the ambient. These pure crystals can then be diffused to prepare the p-n junction.

B. DIFFUSION

The diffusion of metallic impurities is negligibly slow below 1700°C. The basic techniques for diffusing boron and aluminum (both p-type dopants) into n-type SiC have been developed[5] and the diffusion parameters determined. Since the diffusion takes place from 1800°C to 2100°C, it is necessary to provide an atmosphere of SiC around the crystals to prevent decomposition.

As will be discussed later, diffusion depths in the crystals of 10-20 microns were desired for the solar cell studies. This required diffusion times of 10-20 hours at about 1900°C.

The furnace used for diffusion was essentially the same as used for crystal growth. The crystals were placed in a small graphite holder and packed into a crucible surrounded by the dopant (in all cases boron carbide) and SiC grain. No decomposition of the surface was noticeable after the diffusion.

C. MECHANICAL PROCESSING

With both the grown junction and diffusion techniques, a crystal having a bulk of one conductivity type with a surface of the opposite conductivity was obtained. That is, the crystal had a p-n-p (or an n-p-n) structure. To fabricate a p-n junction cell one of the junctions and the edges were removed by cutting or lapping. Due to the hardness of SiC, boron carbide or diamond is used as the abrasive material.[6]

D. CONTACTING

Gold-tantalum alloys which melt near 1100°C are used to make ohmic contacts to SiC and to attach contacting plates or grids. In previous work[5], [6], [7] a number of other alloys and metals have been studied, but thus far Au+5 at. %Ta has been the most successful contact material. SiC has a low thermal expansion coefficient and tungsten (which nearly matches the thermal expansion of SiC) must be used for mounting and contacting plates to prevent crystal fracture during thermal cycling.

The first photodiodes were fabricated using a small (0.020" dia.) tungsten dot for a top contact with a larger tungsten disk for the bottom mounting plate. This top contact is generally sufficient for evaluation, but it is probably an inefficient collector of the generated photocurrent and adds to the series resistance of the cell.

To improve the collection efficiency, studies were made of the feasibility of bonding tungsten mesh to the top surface.

The tungsten mesh used in this evaluation had a 4 mil line-width on 42 mil centers, giving an 82% optical transmission. The problem was to see if this mesh could be uniformly brazed to the SiC crystal with the standard gold-tantalum alloy; with subsequent Al_2O_3 sandblast removal of the excess gold.

The procedure consisted of building up a brazing stack of a tungsten bottom contact, the Au-Ta braze preform, the SiC crystal, another Au-Ta braze preform, and the 5 mil thick tungsten mesh. Pressure is applied to the stack by placing a thin (2-5 mil) carbon sheet over the tungsten mesh and then a spring loaded hold-down over this.

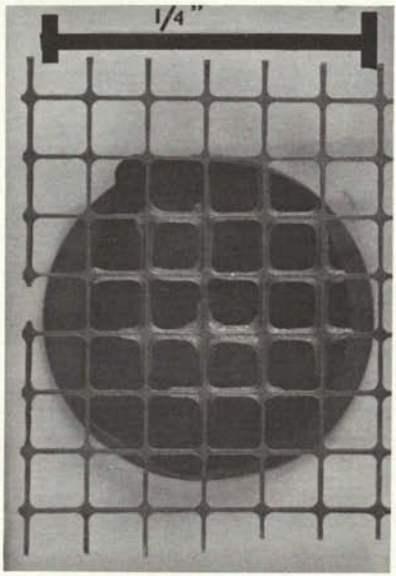

FIGURE 7. SiC Solar Cell WUV-276 Showing Brazed-on Tungsten Mesh

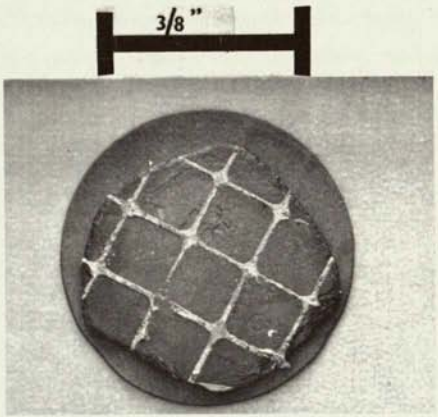

FIGURE 8. SiC Solar Cell WUV-261 Showing a Conductive Epoxy Grid Top Contact

After vacuum brazing (approximately 1200°C), the thin carbon sheet (now attached) and the gold alloy, between the spaces of the tungsten mesh, are removed by a sandblast procedure utilizing an Al_2O_3 abrasive which does not affect the SiC.

These brazed-on grids were tested on both large and small area crystals and no problem was encountered in removing the excess braze on the top surface and around the edge of the crystal (which shorted out the junction). However, on shallow junction crystals (junction depth ~5-8 microns) the braze tended to alloy through and short out the junction. On these crystals the grid was attached using a high temperature (300°C) conductive epoxy. After curing the epoxy, the tungsten grid could be lifted off leaving a gridded top contact of conductive epoxy. Examples of these two techniques are shown in Figures 7 and 8.

The gridded structure led to a distinct improvement in both the open circuit voltage and the short circuit current as well as the maximum power. This would indicate that both the collection efficiency and the series resistance was decreased. Figure 9 shows the comparison curves for WUV-246 at 100°C with a dot contact and a mesh contact. Both the open circuit voltage and short circuit current increased by about 20% while the maximum power increased by about a factor of two.

A detailed study of interconnection methods was not carried out. However, to test the response of several solar cells in parallel and in series configurations, several units were connected using thermal compression bonded gold wire. This bonding could be made either to the small amount of gold remaining around the edge of the tungsten mesh or to the epoxy grid. A prototype solar cell panel could be interconnected in this manner.

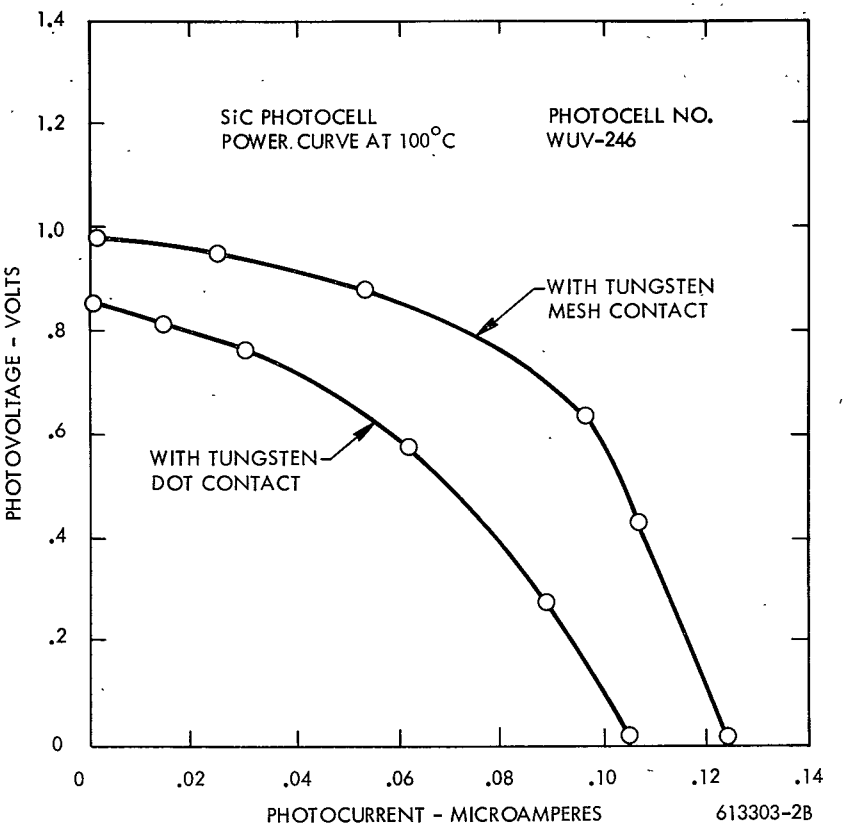

FIGURE 9. SiC Solar Cell WUV-246; Comparison of Current-Voltage Curves at 100°C with Tungsten Dot Contact and Tungsten Mesh Contact; Tungsten Source, ~55 mw/cm^2 Intensity

E. ANTI-REFLECTION COATING

Due to the high index of refraction of SiC (approximately 2.7 near 4000 Å), reflection losses could approach fifty percent. Thus an anti-reflection coating stable to 400°C, with good U.V. transmission would be highly desirable. A possible candidate is aluminum nitride (AlN). AlN has a high band gap and is therefore transparent to U.V. light. Additionally, its index of refraction is intermediate to air and SiC and it is stable to at least 500°C.

A materials group at the Westinghouse Research Center, is presently working on deposition of AlN, BN, etc., and agreed to coat a SiC solar cell[8]. A SiC solar cell was measured as to spectral response and power output. This cell was then sent to the Westinghouse R&D Center and coated with AlN during one of their standard reactive sputtering runs.

Upon retesting the unit, it was found that no shifts were observed in spectral response. However, the coating was much too thick for an anti-reflection coating and more light was lost by absorption than was gained by reduced reflection losses. AlN is still a good candidate material for this application, but much more work would have to be done in this area.

IV. EXPERIMENTAL RESULTS

A. SOLAR SIMULATOR

A consistent, relative, light source is needed to test the power response of the prototype solar cells. The apparatus constructed consisted of a 275 watt tungsten filament lamp ("sunlamp") mounted in a reflector at the top of a chamber. Inside the air-cooled chamber was a heater stage with an enclosed compartment containing a quartz window at the top. Feedthroughs in the compartment side provided for introduction of an inert gas (argon), two thermocouples, several electrical contacts and hold-down clamps. The unit could uniformly heat a two-inch diameter area to 400°C. The distance from the sunlamp to the sample was adjustable. Measurements on SiC photodiodes which had been previously calibrated and on Si photodiodes showed that at six inches from the lamp there was an intensity of about 55 mw/cm^2. This is an approximate figure, good to about $\pm$ 20%. Of this 55 mw/cm^2, about 5 mw/cm^2 was usable by the SiC; i.e. the intensity of radiation having wavelengths shorter than 4100 Å was about 5 mw/cm^2).

All measurements reported in this section (except the quantum efficiency measurements) were made with this apparatus.

B. QUANTUM EFFICIENCY MEASUREMENTS

SiC photodiodes of about 0.02 cm^2 area, with point top contacts, which had been previously fabricated as ultraviolet detectors, were measured in a spectrophotometer. Measurements of output as a function of wavelength were made from room temperature to 400°C. Using standard cells calibrated at the Westinghouse R&D Center, the spectrometer light source output was calibrated so that detector quantum efficiency could be determined. These are only apparent quantum efficiencies since effects of reflection losses are neglected[9,10]. Figure 10 shows the quantum efficiency of these devices at the wavelength corresponding to peak output as a function of temperature.

Quantum efficiency, as used here is defined as the ratio of current out of the diode to the number of photons incident on the device.

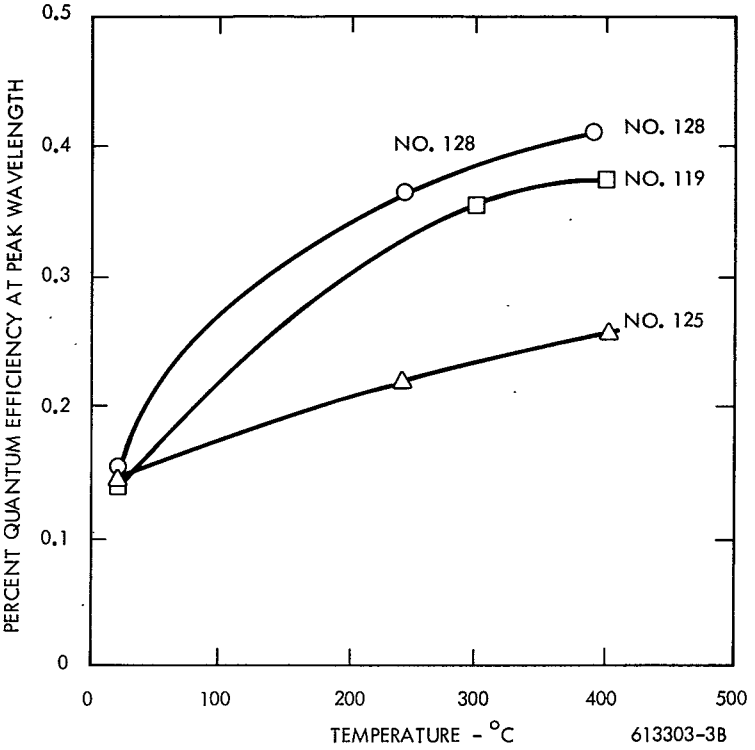

FIGURE 10. Apparent Quantum Efficiency as a Function Of Temperature for Various SiC U.V. Detectors

As can be seen in the figure, the apparent quantum efficiency increases from room temperature to 400°C, which indicates the solar cells should be intrinsically more efficient as current generators at the higher operating temperatures. Impedance measurements on these devices show the impedance decreases approximately four orders of magnitude (viz: 10^{10} to 10^{6} ohms) from room temperature to 400°C.

The quantum efficiencies shown in the figure are representative of devices fabricated throughout the program.

C. FORWARD ELECTRICAL CHARACTERISTICS OF SiC SOLAR CELLS

Later in this section, impedance values of up to 10^{9} ohms are given for the prototype SiC solar cells. This value is much larger than for silicon cells where the impedance is generally less than 1.0 ohm[11]. This high impedance value is partly due to the measurement technique used. The impedance of the SiC cell has been determined using an electronic ohmmeter which employs a small sampling voltage (0.1 to 0.5 volts). This voltage is below the "Turn-on" portion of the diode forward characteristic and the device impedance is thus approximately the same in either the forward or reverse directions (in the high megohm range). However, if a suitable sampling voltage is used, the device impedance is found to be closer to Si units, which usually are measured above their "turn-on" point.

Device WUV-232 (for which power curves are later presented) was evaluated by applying a forward voltage, measuring the forward current, and calculating the drak resistance. Device WUV-232 has an area of 0.03 cm^2 and is typical of many of the cells fabricated early in this program. Table 2 shows the variation of forward current and dark resistance with applied voltage. This resistance value changes from 2×10^{8} ohms at 0.2 volts to 55 ohms at 5.5 volts.

Table 2

Dark Forward Electrical Characteristics of Diode WUV-232
at Room Temperature

Applied Voltage (volts)	Forward Current (A)	Calculated Resistance (ohms)
0.2	1×10^{-9}	0.2×10^{9}
0.4	1×10^{-8}	0.4×10^{8}
0.5	2×10^{-8}	0.25×10^{8}
0.6	5×10^{-8}	0.12×10^{8}
0.7	1×10^{-7}	0.7×10^{7}
0.8	2.2×10^{-7}	0.36×10^{7}
0.9	3.9×10^{-7}	0.23×10^{7}
1.0	6.1×10^{-7}	0.16×10^{7}
1.2	1.5×10^{-6}	800,000
1.4	3.4×10^{-6}	411,765
1.6	6.4×10^{-6}	250,000
1.8	1.35×10^{-5}	133,333
2.0	4.0×10^{-5}	50,000
2.2	1.2×10^{-4}	18,333
2.4	3.4×10^{-4}	7,059
2.6	7.5×10^{-4}	3,467
2.8	1.65×10^{-3}	1,697
3.0	0.0032	937.5
3.2	0.0054	592.6
3.4	0.009	377.8
3.6	0.013	276.9
3.8	0.018	211.1
4.0	0.025	160.0
4.5	0.043	104.7
5.0	0.069	72.5
5.5	0.10	55

D. SOLAR CELL LOADING CURVE MEASUREMENTS

The first measurement circuit of the loading of the SiC solar cells is shown in Figure 11.

The load resistor was variable from ∞ to 10^8 in decades and from 10^8 ohms to 100 ohms in 0.1 decade steps. The SiC diode resistance was measured (without light) with an electronic ohmmeter. From the measured diode photovoltage, the variable load resistor (R_L) and the dark diode resistance, the total photocurrent (internal plus external) for each voltage could be calculated. The electronic volt-ohmmeter uses sampling voltages between 0.1 and 0.5 volts for resistance measurements. The instrument was set at essentially infinite impedance (10^{14} ohms) for the open circuit voltage and the dark resistance measurements so that it would not affect the solar cell characteristics.

A number of problems were experienced in the initial measurements in that spurious voltages and currents were noted with no light on the device. The problem was traced to three areas: first, high contact resistance within the apparatus which was solved by utilizing gold plated contact tabs, between the device and the current pickoff; second, voltage pick-up (heater, line, light, etc.) due to the high impedance of the SiC p-n junction, third, thermo-voltages and currents due to the temperature gradient between dissimilar cables. The last two problems were largely eliminated by using shielded cables throughout and with aluminum foil reflectors to minimize heat pick-up.

With these improvements, it was possible to make reproducible measurements to 400°C using an argon ambient.

An example of the data obtainable using this technique is shown in Figures 12 through 15, which are loading curves for diode WUV-230 at 70°C, 165°C, 265°C and 400°C. In these figures the photovoltage and photocurrent are those measured directly at the terminals of the device.

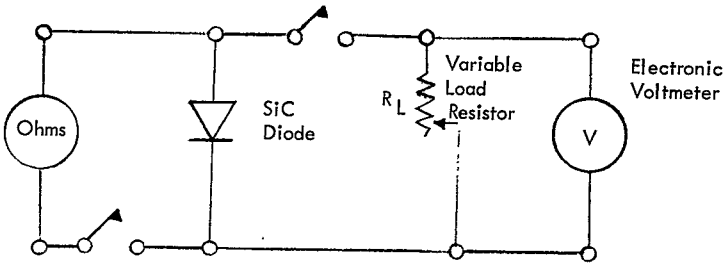

FIGURE 11. Measurement Circuit for SiC Photodiode Loading Curves (No. 1)

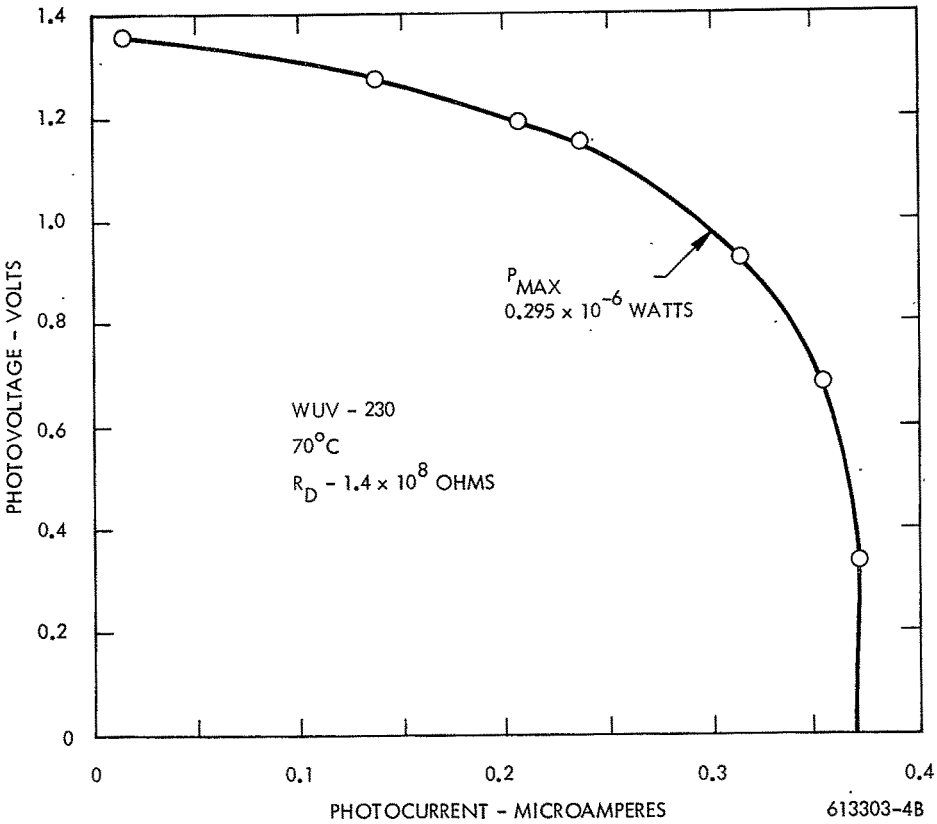

FIGURE 12. Voltage vs. Calculated Total Photocurrent for SiC Photocell at 70°C - Tungsten Source, 55 mw/cm^2 Intensity

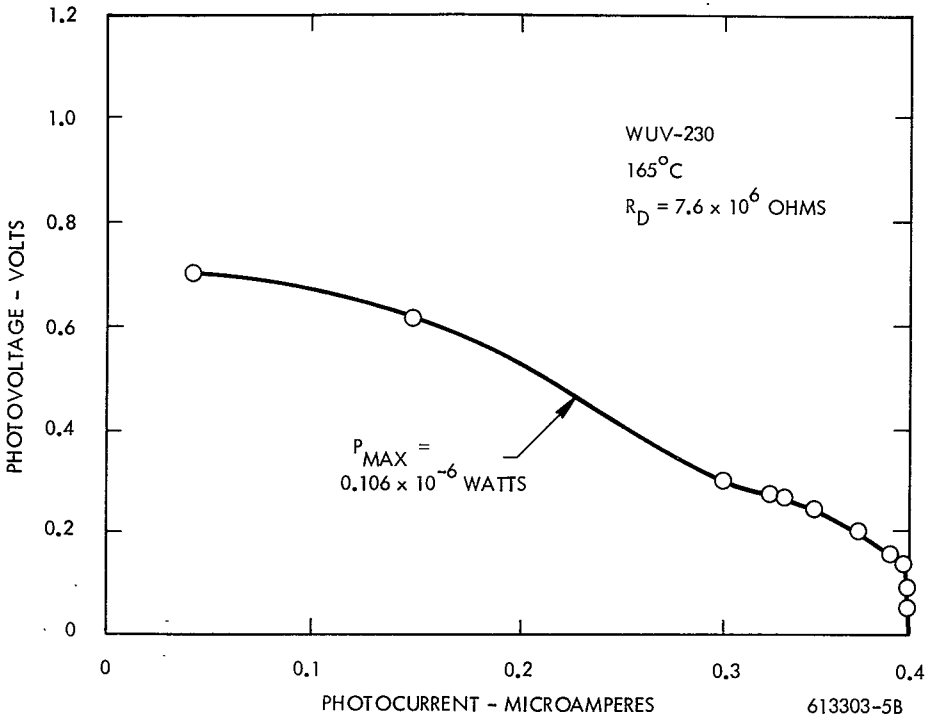

FIGURE 13. Voltage vs. Calculated Total Photocurrent for SiC Photocell at 165°C - Tungsten Source, 55 mw/cm^2 Intensity

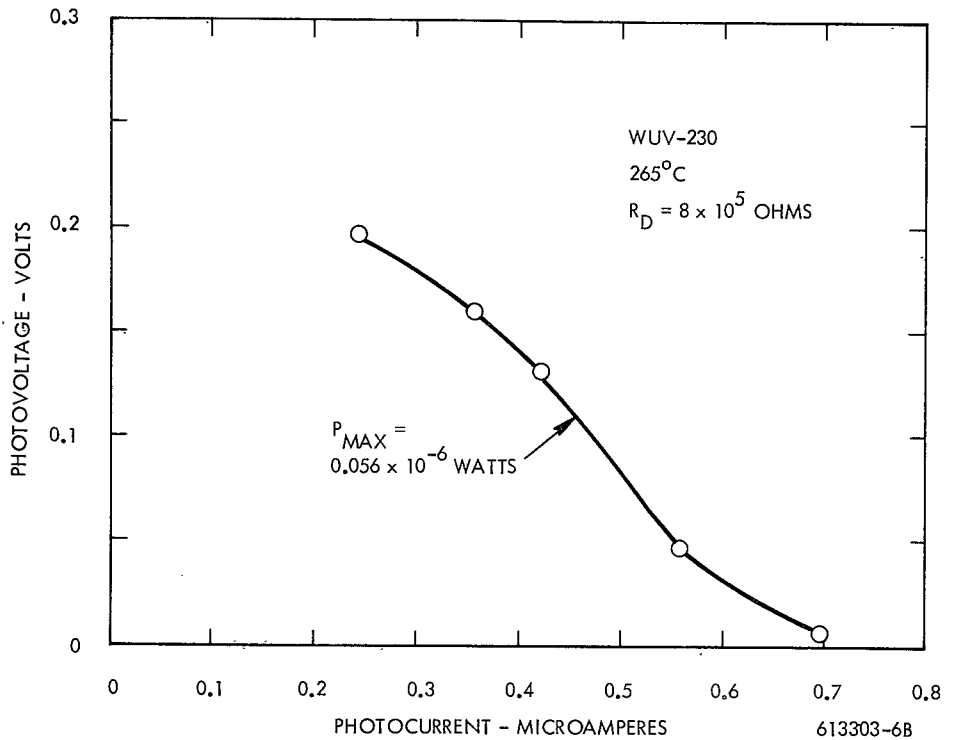

FIGURE 14. Voltage vs. Calculated Total Photocurrent for SiC Photocell at 265°C - Tungsten Source, 55 mw/cm^2 Intensity

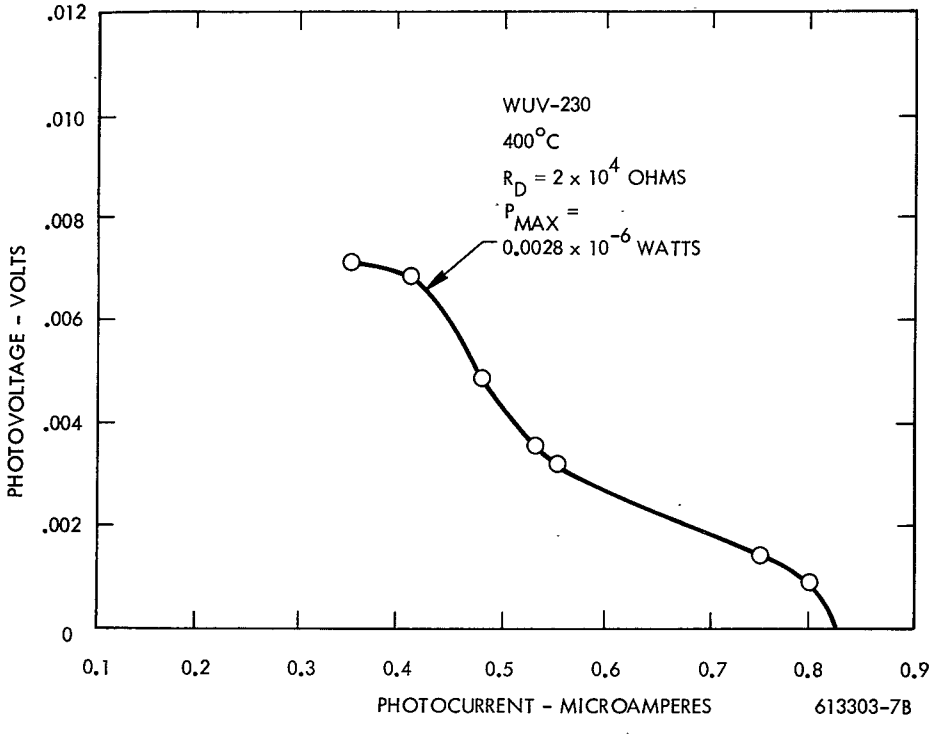

FIGURE 15. Voltage vs. Calculated Total Photocurrent for SiC Photocell at 400°C - Tungsten Source, 55 mw/cm^2 Intensity

As can be seen, as the temperature increases, the open circuit voltage drops rapidly and the short circuit current increases. Additionally, the curves become less square. The maximum power point calculations show a rapid drop in output power with increasing temperature.

These photodiode loading curves show a drastically decreasing power output with increasing temperature, despite the fact that the photocurrent increases with temperature. Several factors are apparent in this decrease. The first and major factor is the decrease in the open circuit voltage with temperature, even though the decrease in band gap is slight (2.9 eV at 30°C and 2.7 eV at 400°C). Second, the device impedance (i.e. the dark resistance across the junction) decreases exponentially with temperature increase. Third, the leakage current, calculated by dividing the open circuit voltage by the junction resistance, increases exponentially.

Figure 15 is a double plot of device impedance and leakage current as a function of temperature for photodiode WUV-230. This figure graphically shows the exponential character of these changes.

Figure 17 is an electronic model of a solar cell. This model is much simpler than considered by Friedlander et al[11].

I_g is an infinite impedance current generator; R_s is the integrated series resistance which includes sheet; contact and spreading resistance terms, and R_p is the parallel or shunt resistance across the junction.

It is easily seen that in the case of SiC, R_p decreases exponentially with temperature which "self loads" the current generator, dropping the voltage and causing a significant internal leakage current. For example, in Figure 12, if we impose the 400°C leakage current of about 0.37 microamperes, we see that the corresponding voltage is virtually zero as was the case at 400°C (V_{oc} = 0.007 V at 400°C). The flattening of the loading curves with temperature would be due to an increase in R_s.

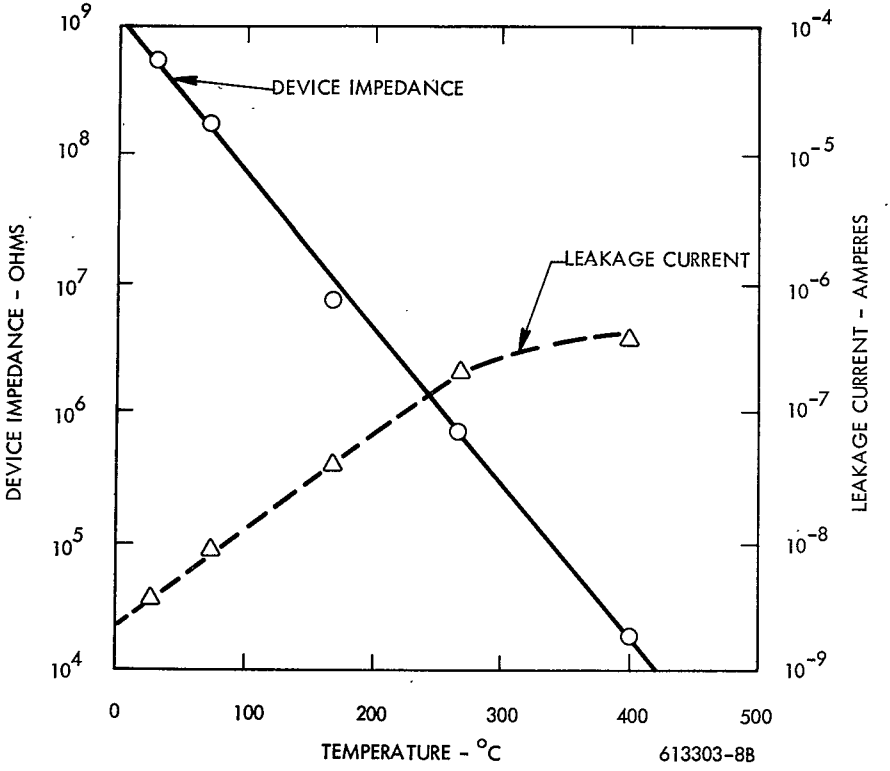

FIGURE 16. Device Impedance and Leakage Current Versus Temperature for Photodiode WUV-230.

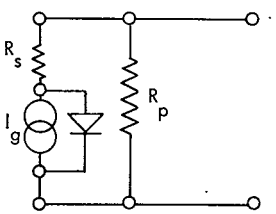

613303-10B

FIGURE 17. Simplified Electronic Analog of a Solar Cell

Since this parasitic current leakage has such a strong effect on cell power output, it would seem that this is the major problem to be overcome for effective operation of SiC solar cells at high temperatures. It should be possible to grow graded junctions with a high enough room temperature R_p (at least 10^{11} ohms) that the 400°C junction leakage current will not severely self load the cell.

As it stands, R_p at 400°C is near 10^4 ohms, each order of magnitude increase in R_p should decrease the leakage current by half an order of magnitude, raising the V_{oc} and power output of the cell.

This measurement technique was valuable in that it permitted us to observe the effects of "self loading" (due to junction leakage current) of the diode. This self-loading shows in the figures that the current is not zero at open circuit voltage. This current at open circuit voltage represented the internal current of the cell.

To determine a more realistic power curve (which would indicate that actual current obtainable from the cell) the measurement circuit was changed to that shown in Figure 18.

The current flowing in the circuit external to the SiC photodiode is measured by the voltage drop across R_l. This resistance is small compared to the variable load resistor R_L, but can be accounted for as short circuit conditions are approached. The measured IV curves then give the actual power output of the SiC cells.

E. MEASUREMENTS ON GROWN AND DIFFUSED JUNCTIONS

Loading curve measurements (from 30°C to 400°C) were made on a series of grown junction crystal runs. These crystal structures varying from quite abrupt to highly graded. The main objective was to investigate the effect of the various junction structures on the parasitic leakage current (as discussed above) and to determine the optimum junction structure.

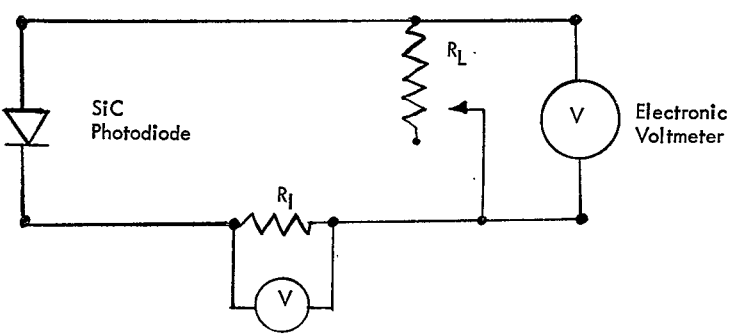

FIGURE 18. Measurement Circuit for SiC Solar Cell Loading Curves (No. 2)

Results indicated that highly graded junctions such as photodiode WUV-244 (Figure 19) have high initial photovoltages which are the least reduced by temperature increase of any type of junction looked at to date. However, WUV-244 had a small photocurrent response, and the photovoltage fell considerably above 250°C. This unit had a relatively low forward voltage for a highly graded junction and this is perhaps the reason for the losses above 250°C.

Figures 20 and 21 show the more typical unit (WUV-232) which increases in current (by a factor of 3) and decreases in voltage by a factor of 30 in going from room temperature to 420°C. This is also the unit for which the room temperature forward electrical characteristics were presented.

Figure 22 shows the I-V curves typical of very abrupt junction structures. The initial photovoltage is small and drops rapidly, but the photocurrent is very large compared to the graded junction. This high photocurrent also increases by a factor of 5.5 between room temperature and 400°C.

Thus, the highly graded junction hold the voltage best, but suffer from low photocurrent output, and the abrupt junctions have large photocurrents, but small photovoltages. Since the most loss of power is due to the extreme voltage decrease, it would seem that the best compromise would lie in the direction of graded junctions. The flatness of these curves above 250°C, of course, indicates high series resistance, but this can be partially alleviated by gridded top contacts.

Within the scope of the program, we were not able to grow junctions having what were believed to be optimum properties. Effort was then spent preparing graded structures by diffusion. In this process, described earlier, lightly doped n-type crystals (10^{17} - 10^{18} carriers/cm^3) are diffused with boron or aluminum at 1900 - 2000°C.

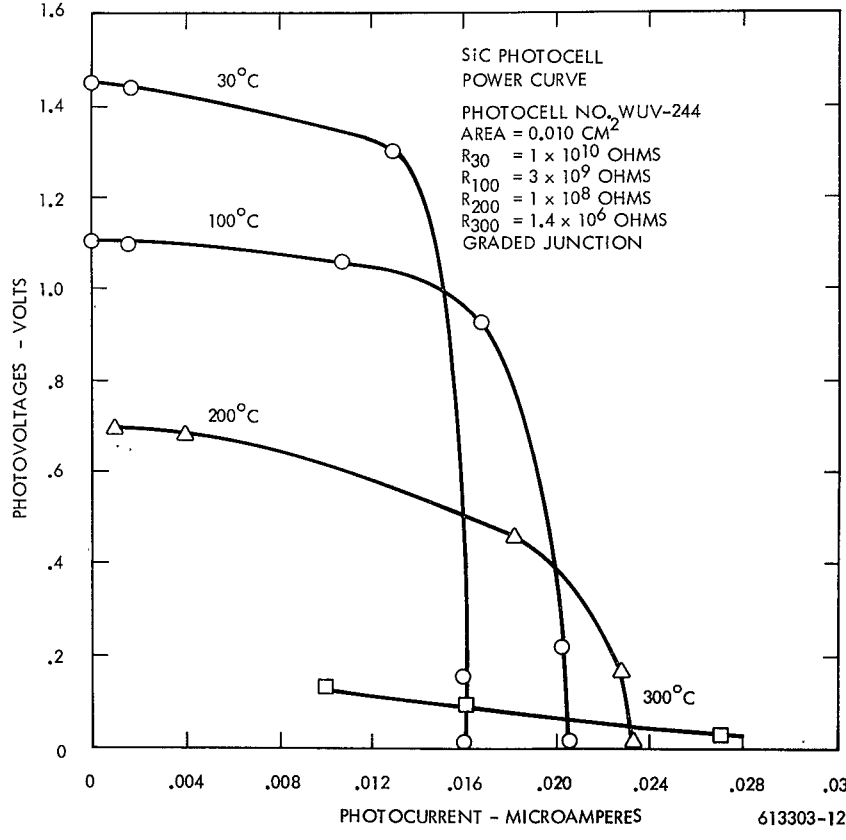

FIGURE 19. Voltage Versus Current for SiC Photocell WUV-244 from 30°C to 300°C
Tungsten Source, ~ 55 mw/cm^2 Intensity

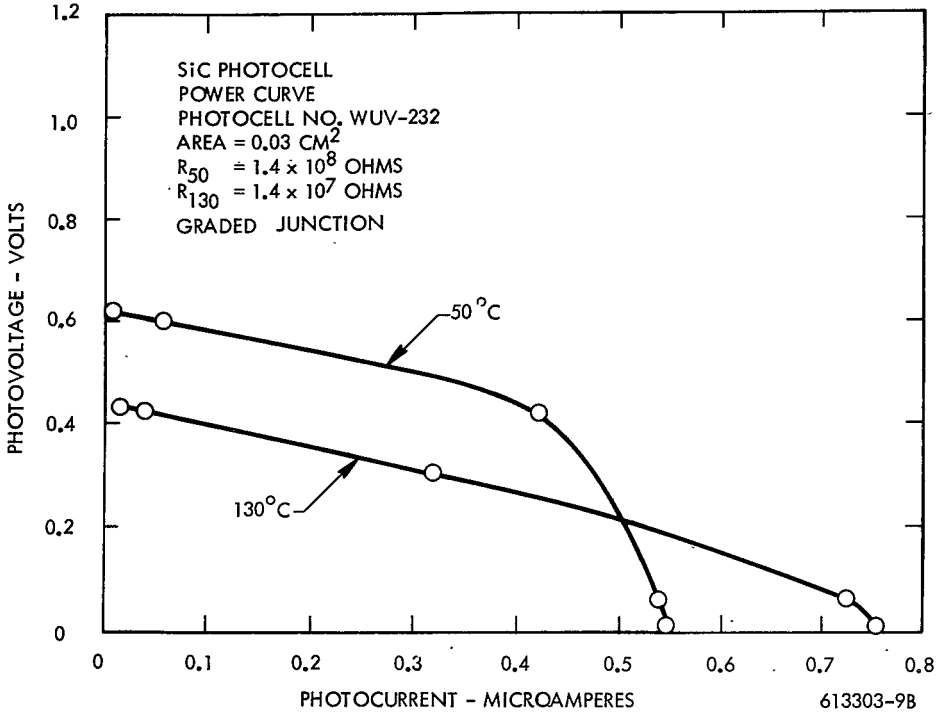

FIGURE 20. Current Versus Voltage for SiC Photodiode WUV-232 from 50°C to 130°C Tungsten Source, ~55 mw/cm^2 Intensity

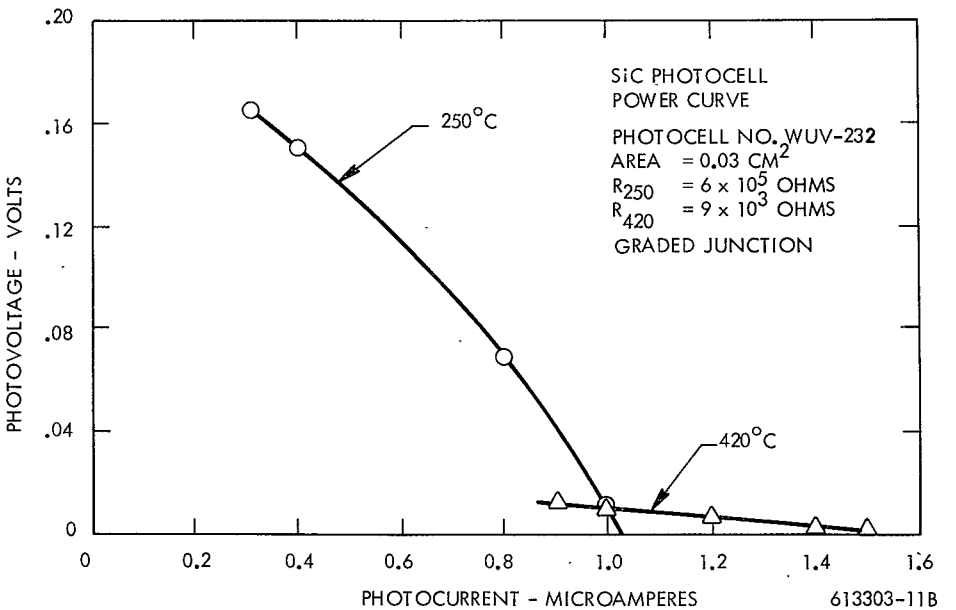

FIGURE 21. Current Versus Voltage for SiC Photodiode WUV-232 from 250°C to 420°C Tungsten Source, ~55 mw/cm^2 Intensity

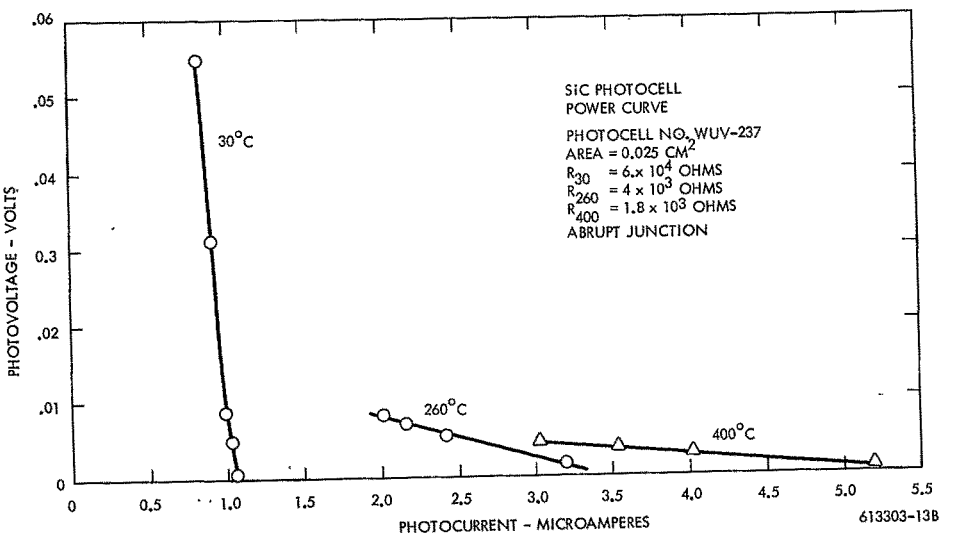

FIGURE 22. Current Versus Voltage for SiC Photodiode WUV-237 from 30°C to 400°C
Tungsten Source, ~ 55 mw/cm² Intensity

Such diffused junctions then are good possibilities for SiC solar cell application. An advantage of the diffusion process is that practically the entire crystal can be utilized, giving the possibility of larger area cells. Disadvantages are that the surface concentration of p-type dopant is limited to about 10^{19} carriers/cm^2. This means that only lightly doped n-type base crystals can be used, and the resulting series resistances of such cells will be much higher than corresponding grown junction crystals.

Several solar cells were made from diffused junction crystals, and they did indeed have very high photovoltages, which held to higher temperatures than any other types previously evaluated.

Figures 23 shows the results from a typical diffused junction solar cell (WUV-202). As can be seen, the voltage remains quite good to nearly 200°C, and as expected, the series resistance appears to be high.

Table 3 shows the temperature coefficient of the photovoltage of these devices. The greatest decrease in the photovoltage occurs between 30°C and 250°C. Although the rate of decrease becomes less above 250°C, the absolute value of the photovoltage by this time is quite low.

Conversly, the temperature coefficient for the abrupt junction is less than for the graded junction, but the absolute value of the photovoltage is much lower.

Since the data indicated that the optimum junction structure appeared to be a graded junction about 15μ deep produced by diffusion, the next approach was to diffuse as large a crystal as possible to maximize the size of the individual photodiodes.

Utilizing large area SiC single n-type crystals (approximately 1/4" diameter) diffused junctions were made with boron as the p-type dopant. These junctions were made deep enough so the spectral response of the cells was a maximum near 3800 to 4000 Å. The crystals were then lapped to leave a p-n junction, brazed to a tungsten disc and the shorting edges removed by a boron carbide sandblast.

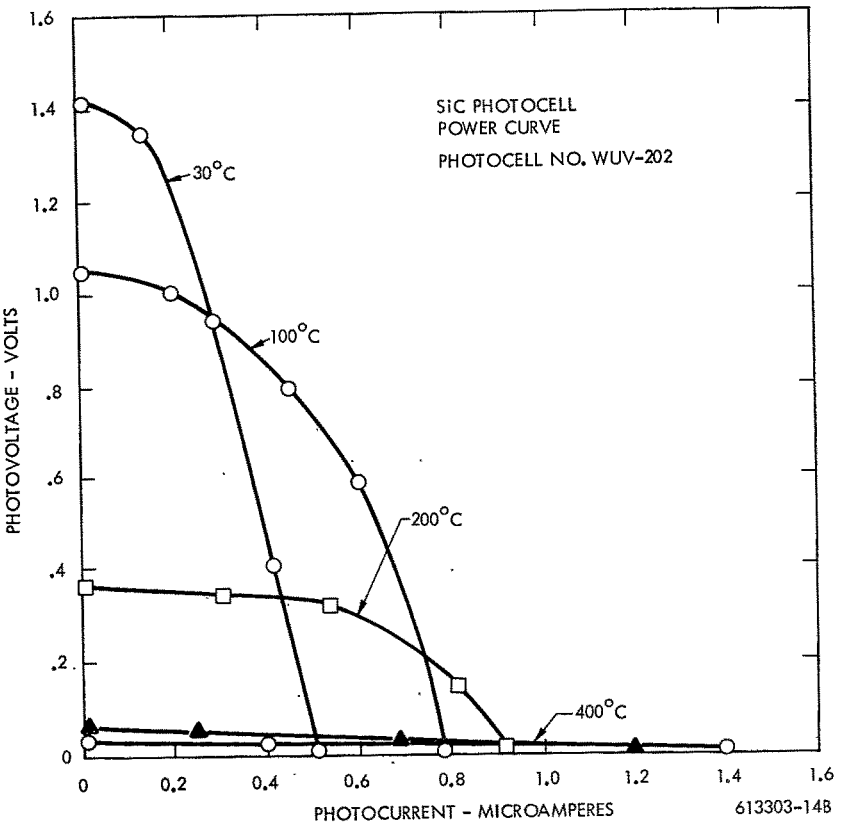

FIGURE 23. Current Versus Voltage for SiC Photodiode WUV-202 (Diffused Junction) from 30°C to 400°C - Tungsten Source ~ 55 mw/cm^2 Intensity

TABLE 3

Temperature Coefficient of Photovoltage of SiC Photodiodes Having Different Junction Structures

Temperature Range (°C)	Temp. Coefficient of Photovoltage (mv/°C)	Device Type
WUV-244		
30-100	4.6	Diffused Junction
100-200	4.0	(graded)
200-300	5.3	
WUV-232		
50-130	3.3	Typical Diffused
130-250	3.2	Junction (graded)
250-420	1.0	
WUV-237		
30-260	0.2	Abrupt Junction
260-400	0.05	
WUV-202		
30-100	5.3	Diffused, Graded
100-200	7.0	Junction
200-300	2.9	
300-400	0.2	

Both brazed-on tungsten mesh and conductive epoxy top contacts were successfully applied to these large area crystals. Early cells tested had an area of 0.01 to 0.03 cm^2, whereas these units had areas a factor of ten larger, with power outputs similarly increased. Since no problems were encountered with fabrication of these cells, a large area SiC solar cell panel seems feasible. Figures 7 and 8 shown earlier show two typical operational cells with a brazed-on tungsten mesh (good to 1000°C - operable to 400°C) and a conductive epoxy grid (good and operable to 300°C).

The current-voltage curves for several of these cells is shown in the next section dealing with series and parallel measurements.

F. SERIES AND PARALLEL OPERATION OF PHOTODIODES

Two sets of double cells were selected for series and parallel operation. One set (WUV-276 and WUV-274) had almost identical impedances (at room temperature), and the other set (WUV-277 and WUV-278) had an order of magnitude mismatch in impedance. Figures 24 to 28 and 29 to 33 are for the matched diodes in series and parallel respectively.

These large area matched units behave pretty much as expected for series and parallel connection, and indicates that a large area solar cell panel is entirely feasible. The mismatched cells did not show significantly different results and no parasitic self-loading effects were noted. Figure 34 is typical of these mismatched units, and shows the individual curves and both the series and parallel connected cells at 200°C. Thus it seems that matching of cells in an array would not be critical to its performance.

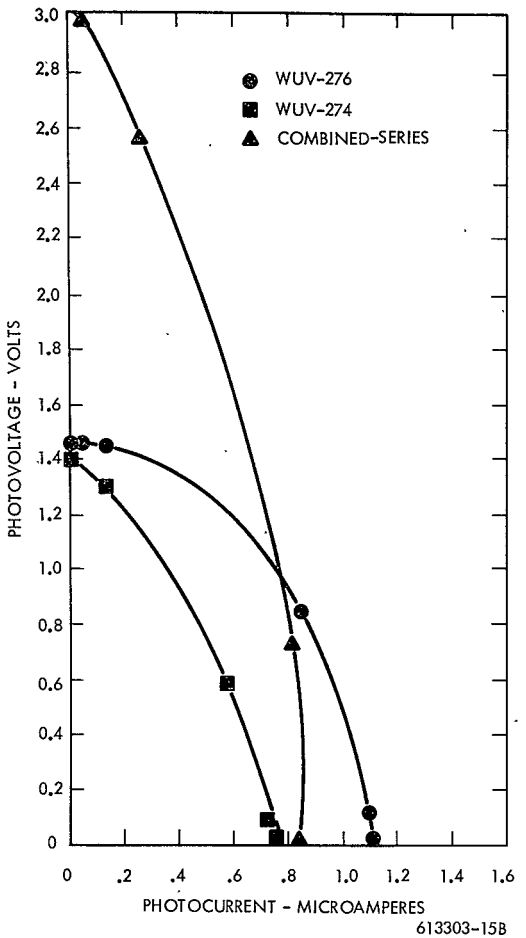

FIGURE 24. Matched SiC Solar Cells in Series at 30°C
Tungsten Source ~55 mw/cm^2 Intensity

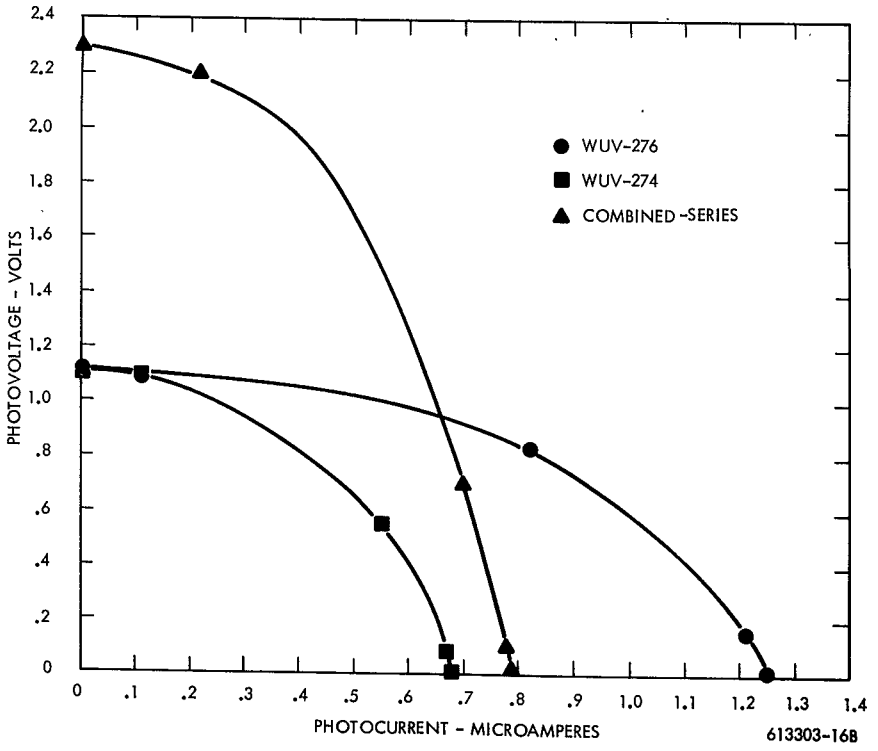

FIGURE 25. Matched SiC Solar Cells in Series at 100°C
Tungsten Source ~55 mw/cm^2 Intensity

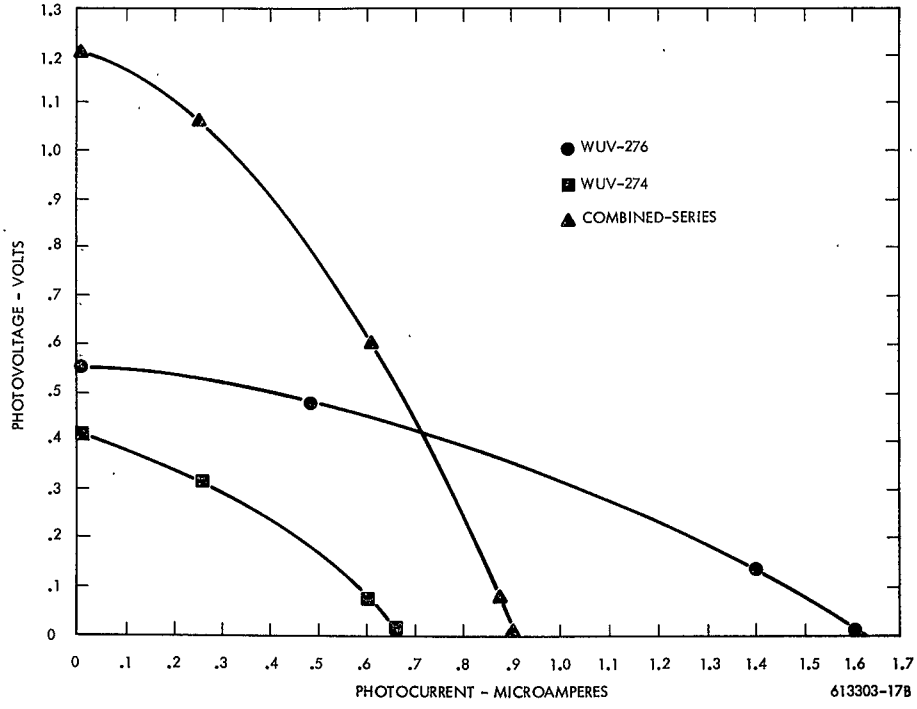

FIGURE 26. Matched SiC Solar Cells in Series at 200°C
Tungsten Source ~55 mw/cm^2 Intensity

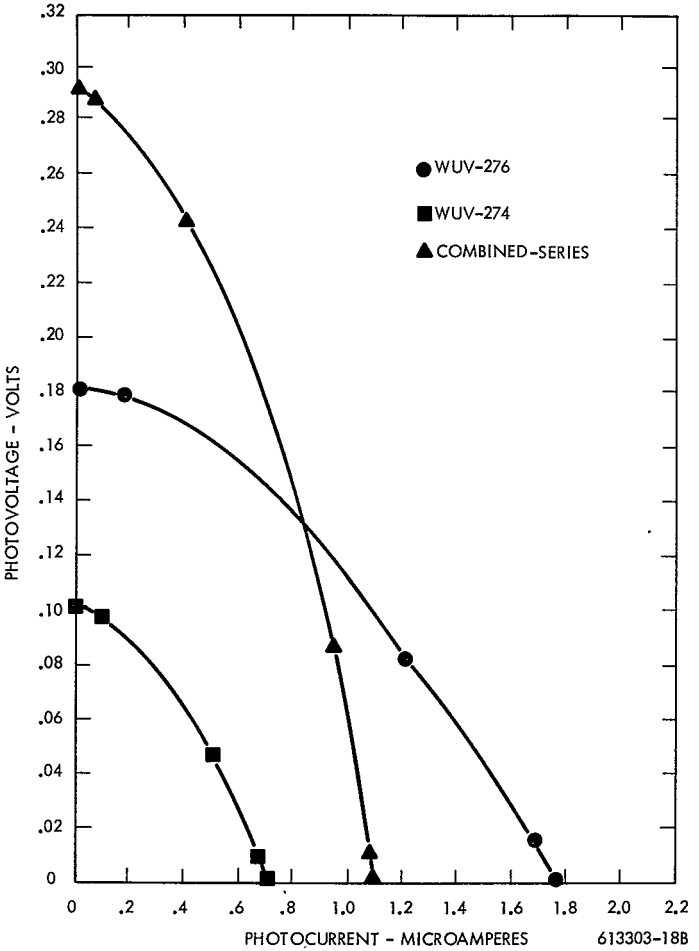

FIGURE 27. Matched SiC Solar Cells in Series at 300°C
Tungsten Source ~55 mw/cm^2 Intensity

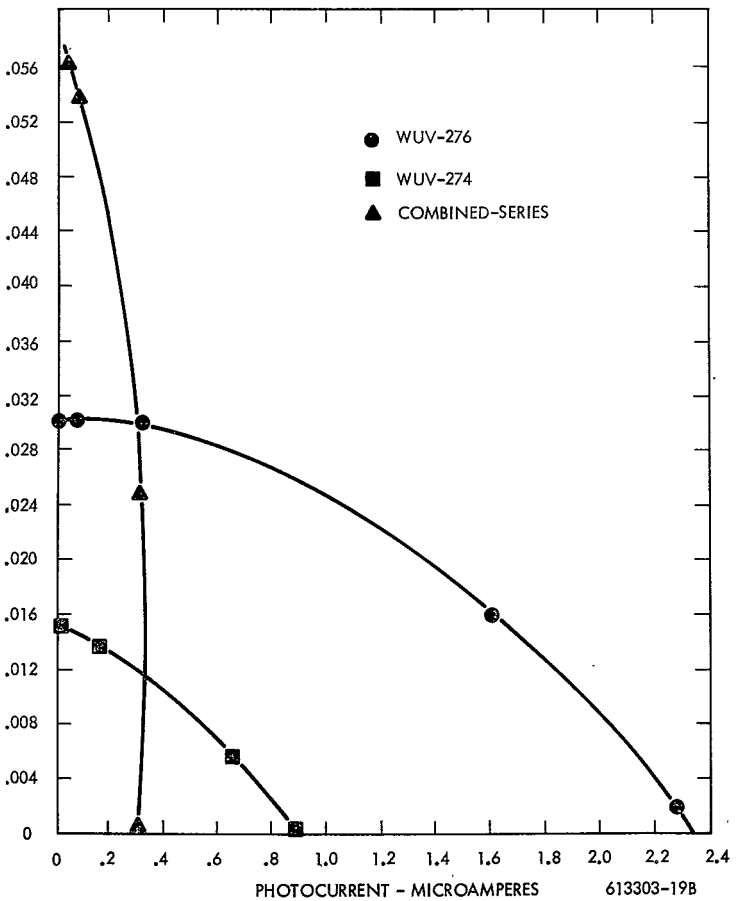

FIGURE 28. Matched SiC Solar Cells in Series at 400°C
Tungsten Source ~55 mw/cm^2 Intensity

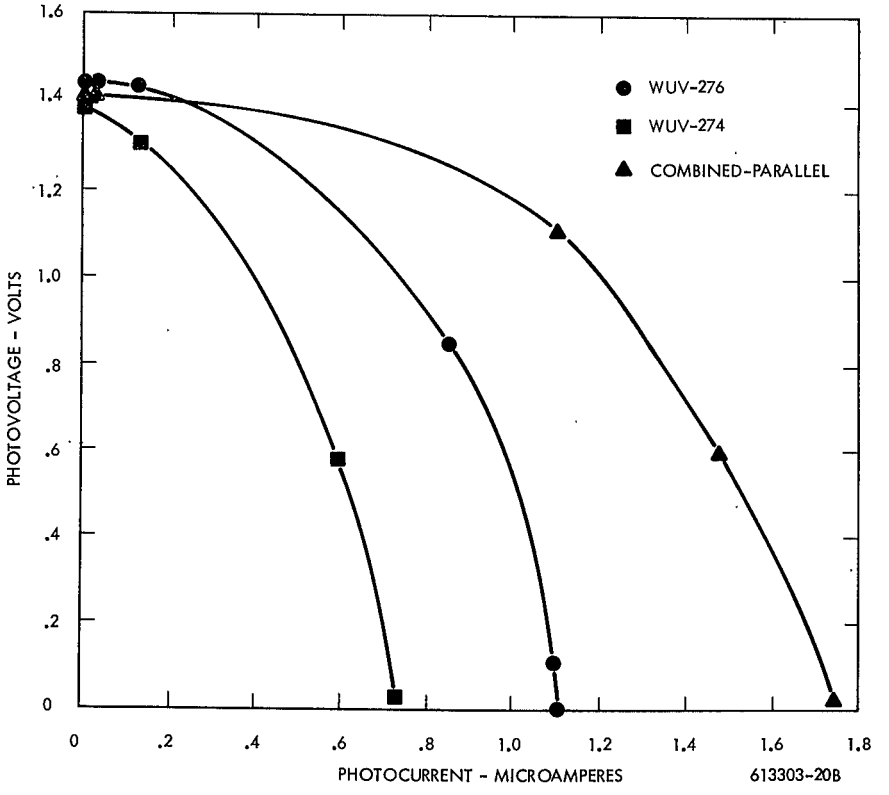

FIGURE 29. Matched SiC Solar Cells in Parallel at 30°C
Tungsten Source ~55 mw/cm^2 Intensity

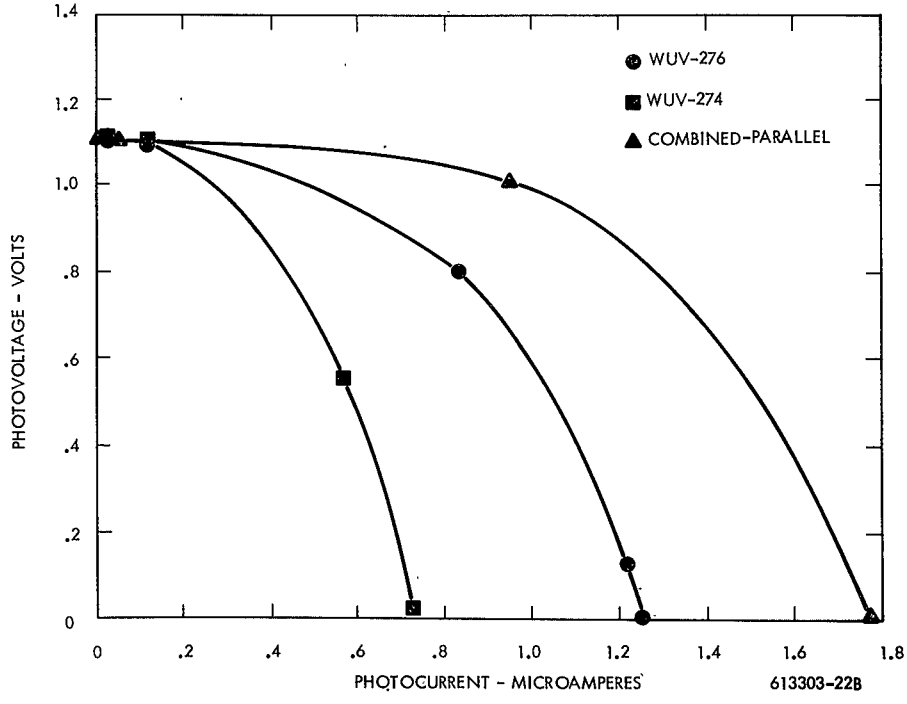

FIGURE 30. Matched SiC Solar Cells in Parallel at 100°C
Tungsten Source ~55 mw/cm^2 Intensity

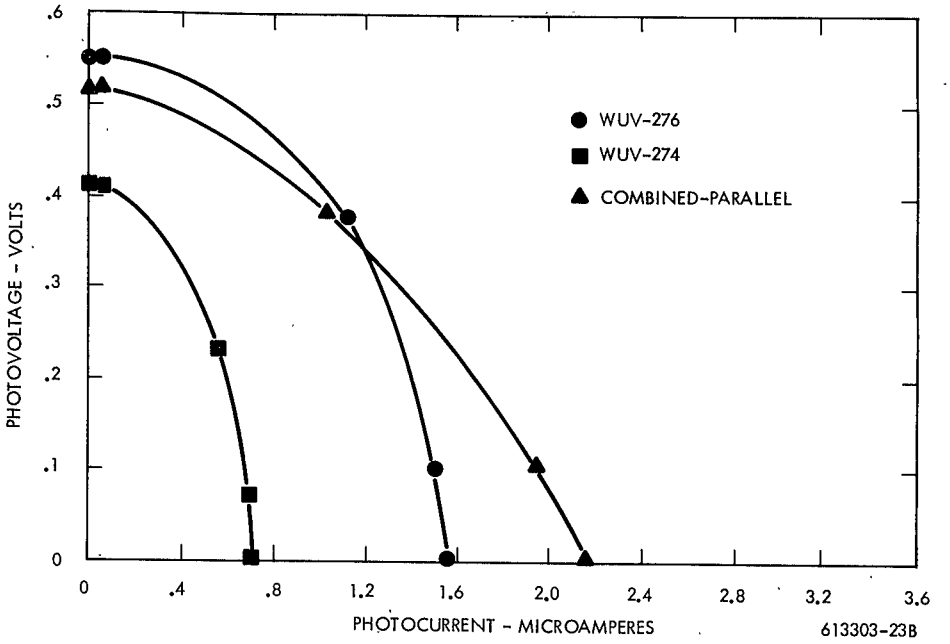

FIGURE 31. Matched SiC Solar Cells in Parallel at 200°C
Tungsten Source ~55 mw/cm^2 Intensity

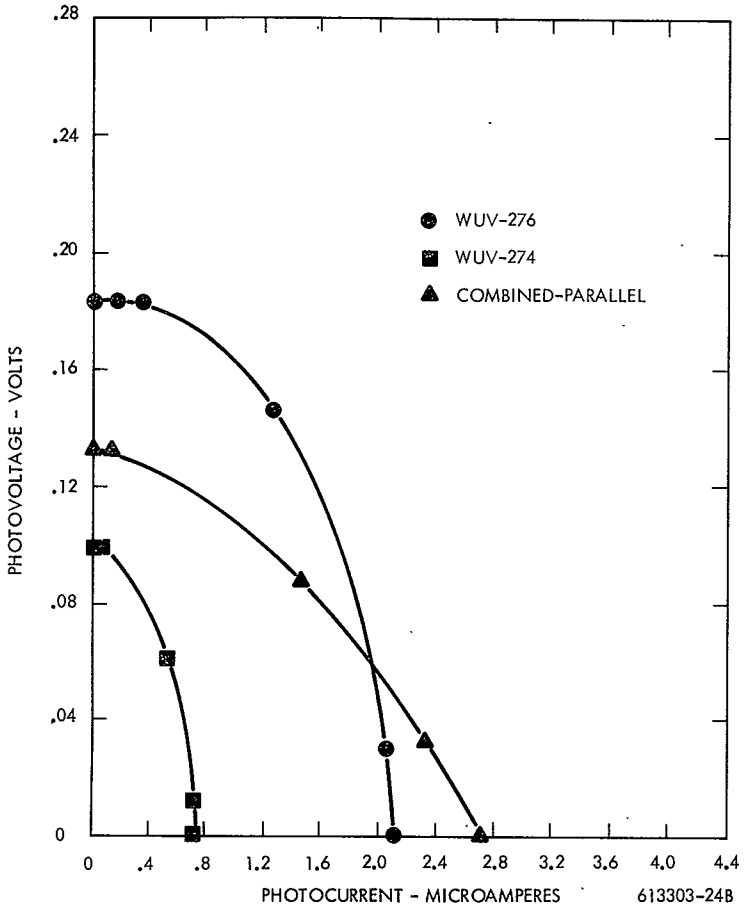

FIGURE 32. Matched SiC Solar Cell in Parallel at 300°C
Tungsten Source ~55 mw/cm^2 Intensity

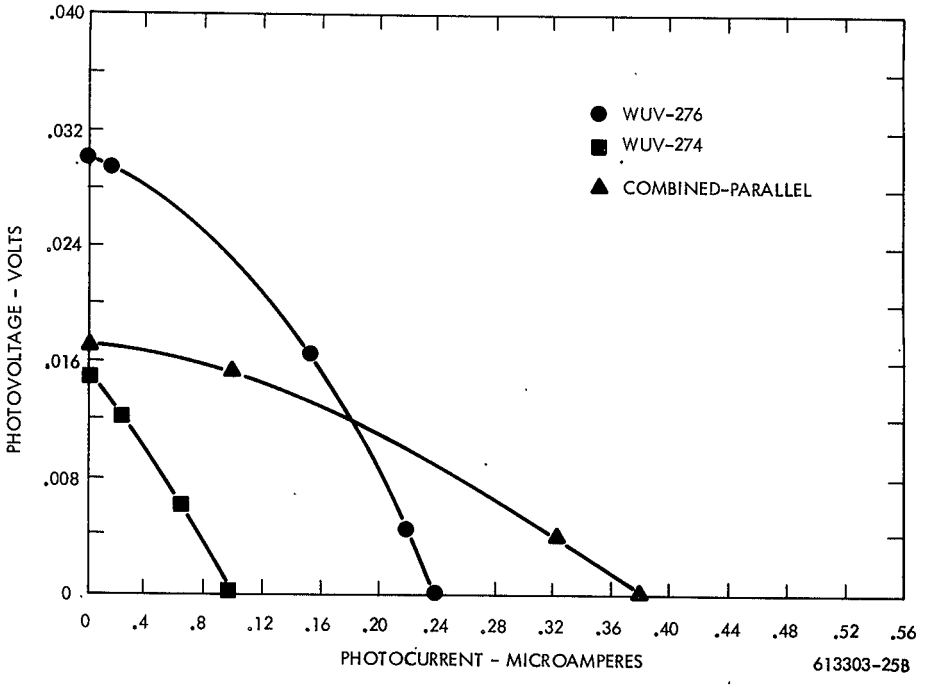

FIGURE 33. Matched SiC Solar Cell in Parallel at 400°C
Tungsten Source ~55 mw/cm^2 Intensity

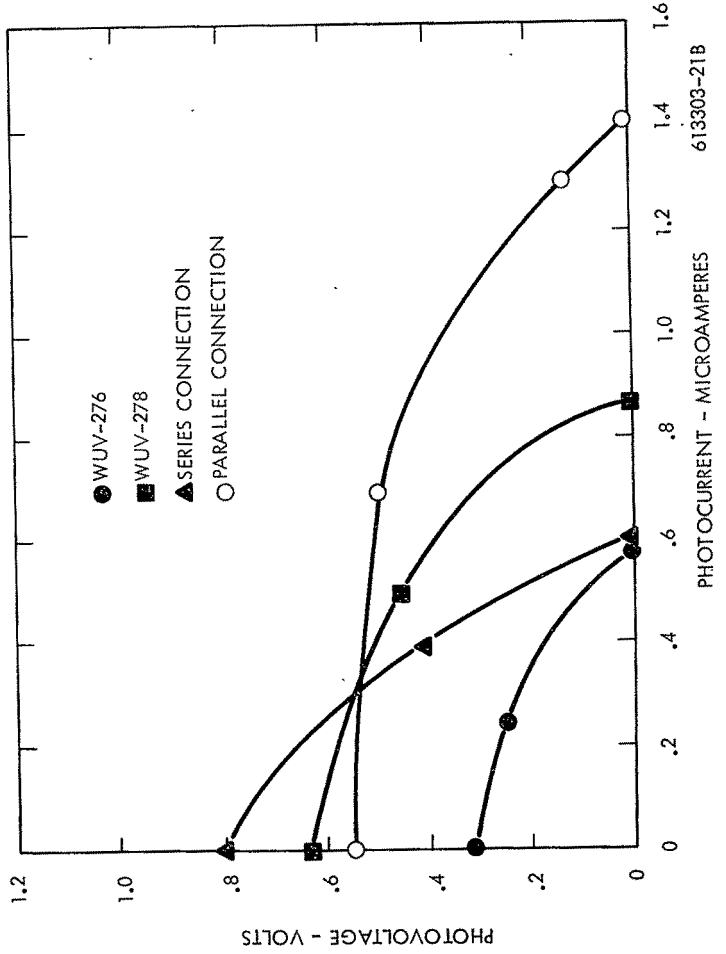

FIGURE 34. Mis-matched SiC Solar Cells at 200°C in Series and Parallel
Tungsten Source ~55 mw/cm² Intensity

G. OPTIMUM OPERATING TEMPERATURE

The measurement of the various SiC solar cell types have all shown the greatest degradation in power output occurs above 250°C. Typically; the open circuit voltage which is the controlling factor, decreases at least an order of magnitude between 200 and 300°C and continues to decrease to 400°C. (See Table 3). Thus, even though these cells operate to 400°C, operation at 200 to 250°C would seem to be an optimum from temperature - power trade-off considerations. The maximum power output (at 250°C) of the SiC cells was nominally 5-15 microwatts/cm^2 at 55 mw/cm^2 input. Under the same conditions (solar radiation at half air mass 1) Si cells have a power output near 7 milliwatts/cm^2. The 10^3 lower power output of the SiC cells is due to: (1) less efficient use of solar spectrum; (2) poor curve shape due to non-optimum contacts, and (3) lower collection efficiency in the diode, (collection efficiency = the fraction of electron hole pairs produced by absorption of light which reach the terminals before being lost at recombination centers in the crystal). In addition to these factors, reflection losses may be as high as fifty percent.

Thus in an SiC cell, utilizing optimum contact geometry and anti-reflection coating, the power output in near Sun missions (e.g. 0.2 AU) should be 25 to 50 times that at 1.0 AU. (At 400°C and 1.0 AU, the power output would be reduced from the 5-15 μ watts/cm^2 to 1-3 μ watts/cm^2).

It should also be noted that if the operational temperature could be held to 250°C or below, conductive epoxy contacts could be utilized and this would greatly simplify panel construction and reduce cost and weight.

H. SAMPLE DIODES DELIVERED UNDER CONTRACT

Table 4 lists the twenty-five (25) diodes delivered under this program. The diode, open circuit voltage, and the impedance as measured at 0.1 volt are also given.

TABLE 4

DATA ON DELIVERED SOLAR CELLS (30°C)
(Tungsten Source ~55 mw/cm^2 Intensity)

Diode Number	Voc (Volts) at 30°C	Isc (Amperes) at 30°C	Area (cm^2)	Resistance (ohms at .1V) at 30°C	Run Number	Contact Type	Max. Power Output (watts) at 30°C
229	0.80	---	0.032	5×10^7	X-178	W DOT	---
233	1.13	1.1×10^{-8}	0.03	3×10^8	X-168	W DOT	$.68 \times 10^{-8}$
243	0.25	1.4×10^{-7}	0.025	2×10^5	X-179	W MESH	0.25×10^{-8}
246	1.20	7×10^{-8}	0.045	4×10^9	X-174	W MESH	1.8×10^{-8}
249	1.40	5×10^{-8}	0.032	10^{10}	X-174	W MESH	2.9×10^{-8}
250	1.05	3×10^{-8}	0.030	2×10^{-9}	X-174	W DOT	1.7×10^{-8}
202	1.40	5×10^{-7}	0.035	4×10^7	AD-41; BD-29	W MESH	0.6×10^{-8}
254	1.15	4×10^{-8}	0.020	7×10^8	X-149	W DOT	2.65×10^{-7}
257	0.80	5.5×10^{-7}	0.075	6×10^8	AD-32; BD-60	Epoxy & Au Dot	1.2×10^{-8}
258	0.25	---	0.10	3×10^8	AD-32; BD-60	Epoxy & Au Dot	1.6×10^{-7}
265	0.60	---	0.20	1×10^7	AD-32; BD-68	W MESH	---
266	0.80	---	0.10	4×10^{10}	AD-34; BD-68	W MESH	---
267	0.62	---	0.20	2×10^9	AD-34; BD-68	W MESH	---
269	1.40	---	0.03	5×10^8	AD-34; BD-68	W DOT	---
272	0.40	---	0.08	1×10^9	RF-26; BD-70	W MESH	---
273	0.85	1×10^{-7}	0.06	7×10^9	AD-39; BD-71	Ag Epoxy	---
274	1.40	7.5×10^{-7}	0.14	8×10^8	AD-39; BD-71	W MESH	4.5×10^{-7}
275	1.20	---	0.14	4×10^8	AD-39; BD-71	W MESH	---
276	1.45	1.1×10^{-6}	0.25	5×10^{10}	AD-34; BD-73	W MESH	8.4×10^{-7}
277	1.30	4×10^{-7}	0.10	1×10^9	AD-34; BD-73	W MESH	2.3×10^{-7}
278	1.45	6.4×10^{-7}	0.18	7×10^8	AD-34; BD-73	W MESH	4.8×10^{-7}
281	1.40	2×10^{-6}	0.27	7×10^8	AD-34; BD-73	W MESH	---
282	1.40	---	0.13	3×10^8	AD-39; BD-71	W MESH	---
283	1.40	---	0.08	6×10^7	AD-39, BD-71	W MESH	---

* X numbers indicate grown junctions
AD-BD numbers indicate diffused junctions

V. OTHER CELL DESIGNS

The work described thus far has dealt only with single junction solar cells. As described earlier, the junction depth of these cells can be optimized by considering the absorption coefficient of SiC at wavelengths longer than the band gap energy and the solar spectrum at air mass zero.

This calculation indicated the junction depth should be near 15 microns with a wide depletion layer. In practice, these depletion layers are difficult to obtain and wide layers lead to a high device impedance due to the bulk resistance of the material. It wasl also shown that due to the temperature variation, in the absorption of radiation in SiC, a cell geometry could be optimized for only one temperature. Thus inevitable trade-offs and compromises are required.

In an effort to surmount these problems, several other cell structures were studied to determine (1) if the cell geometry could be fabricated and (2) what increase, if any, in the efficiency could be obtained.

Structures investigated were (1) multi-junction cell; both constant and varying band gap and (2) a multiple transition cell. In addition, the possibility of fabricating epitaxial cells was studied.

A. MULTI-JUNCTION CELL

A first order theory for two junction silicon cells has been given by Capart[12] and Wolf[13]. Further work has been done by the Westinghouse Research Laboratories[14]. A simple structure is shown in Figure 35 and is essentially taken from the Capart reference.

The justification for even considering such a structure is that it would make more efficient use of the incident radiation. In the case of SiC, radiation with wavelengths between 2200 Å and 4200 Å.

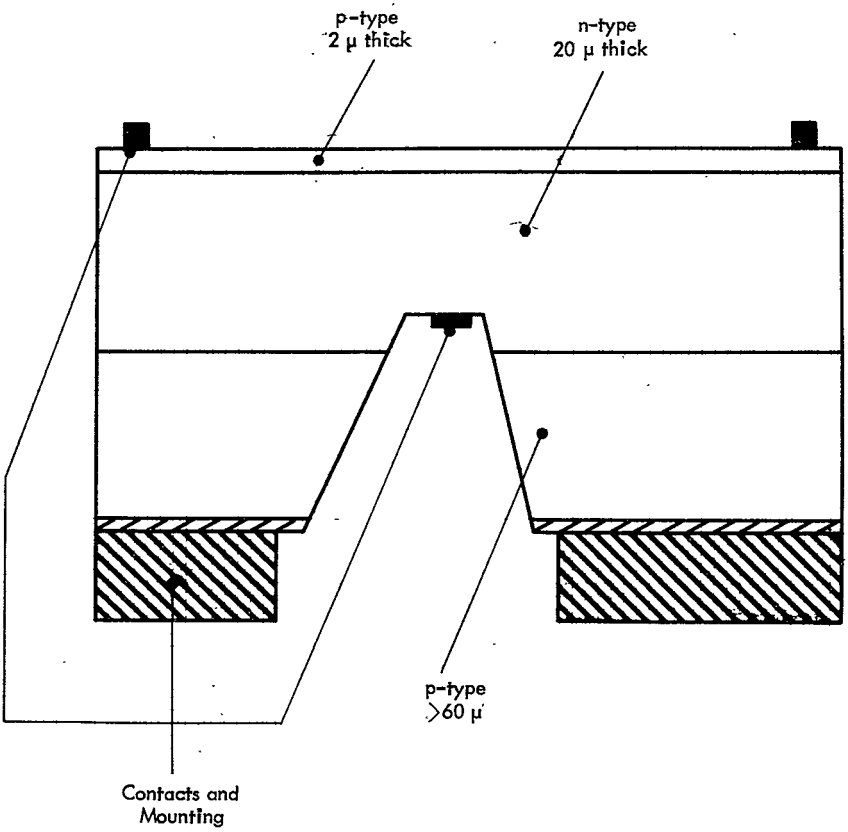

FIGURE 35. Schematic of Multijunction Solar Cell

Capart calculates the spectral response of the two junctions and the efficiency of the cell by asseming various junction depths and base layer thicknesses together with material parameters of diffusion lengths, crystal doping levels etc. Under optimum conditions for a Si cell with a front junction depth of 0.5μ, and a base layer thickness of about 50 microns, he finds there could be a 35% improvement in cell efficiency.

In order to obtain an approximation of the effect of this structure in SiC, the following should be considered: (1) only electron-hole pairs produced in the depletion region will be collected and (2) radiation with wavelength greater than 4200 Å will not be absorbed.

The first condition shows that the junction should have a wide depletion layer to collect the maximum number of electron-hole pairs. The second (See Figure 4) indicates that junction depths greater than 25 microns will not be efficient in that more than 60% of the solar flux with wavelengths shorter than 4200 Å will be absorbed in the first 25 microns. On the other hand, Figure 6 shows that the solar flux increases with longer wavelengths, therefore the maximum number of electron-hole pairs per unit wavelength will be produced by radiation in the 4000 - 4200 Å region. Thus, the second junction should be between 20 to 30 microns deep. Further consideration of Figures 1, 4 and 6 indicates that to absorb the maximum amount of radiation in the 2200 - 3600 Å range, the first junction should be no more than 2 microns deep. For purposes of this approximation, the depletion width of each junction is assumed to be 4 microns.

With a cell of this design, about 65% of the total solar flux between 2200 and 4200 Å would be absorbed. (A larger amount could be absorbed if the depletion width could be increased, but much wider depletion widths would lead to very high resistivity cells and recombination of electron-hole pairs even in the high field layer.)

In a single junction cell with the junction centered at 20 microns, about 50% of the total solar flux would be absorbed. In the above design 30% more electron-holes would be produced in the two junction cells due to the first, shallow junction. There is no a priori reason to suspect that the collection efficiency of the individual junctions would be different from a single junction cell, therefore the total efficiency of the device should be increased by 30%.

Further increases in efficiency would be possible by using a three or even four junction cell, but complexity of geometry, fabrication and interconnection of the junctions would pose an extremely difficult problem.

A cross-section of a two junction cell with appropriate contacts is shown in Figure 35. This configuration could be produced in the following steps.

1. On an n-type crystal at least 200μ thick, diffuse a p-type dopant in 60μ.

2. Lap off "silicon"* side of crystal to remove one p-type layer.

3. Diffuse crystal second time to produce a two micron deep junction on the silicon side. (During this diffusion there will be very little increase in the junction depth on the unlapped side of the crystal.)

4. Using SiO_2 masking and Cl_2 etching[4] etch groove through p-type layer on carbon side of crystal to n-type material. (Etch depth approximately 60 microns).

5. Through appropriate masks, apply sputtered contacts to top p-type surface and bottom of n-type surface.

6. Alloy cell to mounting block (non-conductive).

* SiC is a polar crystal with the two sides exhibiting different properties in etching and oxidation. The sides are called (historically) the "silicon" and "carbon" faces. The silicon face is practically inert to oxidation and gaseous etching.

Steps 5 and 6 are the most critical and would require development. Although shown as single contacts, the top contact and the contact to the n-type surface could be gridded to improve the collection efficiency.

One refinement that could be considered later is to so design the cell that each of the junctions would absorb the same number of photons. This would assure that each layer would conduct current at its maximum power point[13]. In all probability, this could only be achieved in a three or four junction cell.

The above has considered that the entire cell is of one polytype and therefore has one band gap energy. A further increase in efficiency could be obtained by fabricating the second (or third) junction from a lower energy gap material.

The rationale behind this structure is that by fabricating the cell with the second (or third) junction of a lower band gap material, longer wavelength radiation could be absorbed and thus further increase the efficiency of the device (100% efficiency = use of all photon energies in the solar spectrum).

In this report we will consider only cubic SiC and the various polytypes of hexagonal SiC[15].

The following lists the band gaps of the two most common hexagonal polytypes and cubic SiC and the wavelength equivalent of this band gap, ie. the longest wavelength that will be absorbed.

	Band Gap (eV)	Wavelength Equivalent (Å)
6H - Hexagonal SiC	2.9	4250
15R - Hexagonal SiC	2.85	4350
2C - Cubic SiC	2.30	5360

Only a slight improvement would be realized by using a combination of 6H and 15R. However, if we consider a three junction device with the surface junction and second junction being hexagonal SiC and the third junction being β-SiC a larger improvement is noted. By placing the third deep into the crystal, at least 75 microns 70% more photons will be absorbed, which would greatly increase the efficiency of the device.

The fabrication of such a cell would be a difficult problem. The simplest procedure would be to follow steps 1 through 3 as given above. At this point, 25 microns of p-type β-SiC and 50 microns of n-type β-SiC would be deposited by epitaxial deposition. This would be followed by two separate masking and Cl_2 etchs to open contact areas into the n-type hexagonal SiC and p-type β-SiC.

The fabrication as given would be quite complex, but straight-forward. The major advances needed are improvements in the epitaxial deposition of β-SiC on α-SiC at controlled thicknesses and doping levels.

In summary, multijunction SiC solar cells appear to be fabricable based on present state-of-the-art. Increases in efficiency by a factor of 2-3 appear to be possible.

The pyrolytic deposition of SiC is discussed in the next section.

B. PYROLYTIC DEPOSITION OF SiC

SiC can be pyrolytically deposited by the thermal decomposition of carbon tetrachloride and silicon tetrachloride or other suitable compounds, e.g. toluene and silane.

Most of the experimental work reported deals with the deposition of a single crystal SiC layer on a SiC single crystal substrate[18]. This work showed that at deposition temperatures above 1700°C, the deposited layer was of the hexagonal phase while below 1700°C, the

deposited layer was cubic. The perfection of the deposited epitaxial layer was dependent on the substrate preparation and perfection with the best layers being grown on either natural or polished crystal surfaces. On a number of samples, transmission Laue photograms were obtained of both the layer and substrate. Although, generally, the epitaxial layer was of the same polytype as the substrate, in a few specimens the layer was of a different polytype from the substrate.

Both p-type and n-type layers were grown. The n-type layers were produced by adding a small amount of nitrogen, arsine or phosphine to the reactant gas stream while for p-type layers, diborane was added. Several different types of junction structures were grown in that n-type layers were grown on p-type substrate; p-type layers were grown on n-type substrates; and in several experiments, an n-type layer was grown on a n-type substrate followed by a p-type layer. Layer thicknesses of 20-30 microns were nominal.

This work was carried out during programs where the major effort was to fabricate high current rectifiers[6] or transistors[17]. Although the epitaxial layer appeared to be of high perfection from x-ray and etching studies, the junctions were not suitable for either rectifiers or transistors. The specimens were not examined for photo response at that time.

During the course of the present program, a number of these specimens were tested as to their usefulness as solar cells. Two effects were noted. First, on several samples, the contacting alloy shorted out the p-n junction. This was also noted in the earlier programs. Although conclusive evidence is not available, it is suspected that small microcracks and/or pipes in the layer permit the alloy to penetrate further than normal. Second, the specimens which did not short out, were not better or no worse, than the diffused junctions.

Therefore, the present state-of-the-art of the epitaxial growth of SiC on SiC is: 1) single crystal layers of hexagonal SiC and cubic SiC can be grown on hexagonal SiC platelets, 2) the layers can be doped either n-type or p-type, 3) the junction between the substrate and the layer or the junction composed of epitaxial layers shows a photoresponse of about the same efficiency as a diffused junction.

If solar cells are to be fabricated from pyrolytically deposited layers, consideration should be given to depositions on large areas, for examples, sizes equal to or greater than present silicon cells. This would rule out the use of SiC as a substrate material, and in all probability, the deposited layers would be polycrystalline. The loss in efficiency due to the polycrystalline nature of the deposit should be more than compensated by the larger area available.

Polycrystalline layers of SiC have been deposited on SiC substrates using the reduction of dimethyldichlorosilane. In the presence of hydrogen this compound reduces to supply both the carbon and silicon vapor species. Temperatures between 1200 and 1650°C were used with the best coatings being obtained at 1400-1450°C. Above and below this temperature range loosely adherent, powdery layers were obtained.

In the proper temperature range, the layers adhered tightly to the substrate and were composed of elongated rods (long axis parallel to the substrate) or of hexagonal platelets.

The growth rate of these polycrystalline layers was up to 20 mils/hour which is about 20 times the growth rate of the single crystal layers. The interface between the substrate and the epitaxial layer was delineated by edge polishing and chlorine etching. The bonding to the substrate is good, but the surface is sufficiently irregular that a lapping operation would be needed to make use of the top surface.

The pyrolytic deposition of SiC on other than SiC substrates has not been reported. However, from the results of the above, it would appear possible to grow dense, adherent layers on various foreign substrates. Substrates which are immediately obvious as candidates are Al_2O_3, W, etc. depending on whether a insulating or conducting substrate is desired.

C. MULTIPLE TRANSITION CELL

The basic limitation of SiC solar cells is that they utilize only photons having an energy greater than the SiC band gap energy. Thus, something less than 15% of the total solar flux energy is available for absorbtion. The remainder passes through the crystal.

If, for example, an energy level could be inserted 0.2 eV below the conduction band in 6H-SiC, the cell would still absorb wavelengths shorter than 4200 Å ($\approx$ Eg).

In addition, photons of energy $h\gamma$, where $Eg > h\gamma > (Eg - .2\ eV)$ can cause transistions from the valance band to the trap level and additional photons of energy $h\gamma_2$ where $(Eg - .2\ eV) > h\gamma_2 > 0.2$ eV could cause transitions from the trap level to the conduction band. This process has been discussed by Wolf[13] and requires certain assumptions to be operable. First, the trap must be slow so that another photon can interact with the trapped electron. It also assumes that the introduction of a trap level changes the absorbtion characteristics of the material so that the lower energy photons can be utilized.

Thus, the introduction of a trap density of $10^{18} - 10^{19}/cm^3$ Wolf shows that for a semiconductor with Eg = 3 eV, about 3% of the solar photons are utilized in pair production*. With a single trap level the utilization increase to 55% while with two trap levels it further increases to 80%. He also shows that for a semiconductor with Eg = 3.0 eV the optimum trap levels are 1.25 eV up from the valance band for a single trap and 0.6 eV and 1.4 eV up from the valance level for two trap levels.

* This number is different from our data which suggests that about 14% of the solar photons can cause band-band transitions, however, Wolf is using air mass one while we used air mass zero in our calculations. We will use Wolf's figure here for continuity of the argument.

The recombination properties of such a high density of traps have been studied by Shockley[16]. In general, the traps should have small capture coefficient and large emissive coefficients.

Very little is known regarding deep level traps in SiC, and a rather broad theoretical and experimental program would be needed to obtain any definitive answers. However, there is some data which can be interpreted in terms of the existence of deep traps in SiC.

First, in experiments to determine the minority carrier lifetime in SiC[17] carriers were injected into crystals at several different frequencies. These carriers will recombine with holes in the bulk material and give rise to recombination radiation. By determining the frequency at which the recombination radiation goes to zero (i.e. carriers injected and retracted from the bulk before they recombine) an idea of the carrier lifetime can be obtained.

It was noted that the color of the recombination radiation varied from green to red (no attempt was made to detect infra red), and in many crystals several different colors were noted. In these cases, the different colors disappeared at different frequencies. Although these were only preliminary experiments, the different colors were interpreted to indicate different recombination level centers, and therefore rather deep trap levels. It would be instructive to repeat these experiments to determine if there are recombination levels in the infra red region ($E < 1$ eV).

Experimental data on the spectral response of a few photodiodes also suggests trap levels. Usually on SiC devices, there is little if any response above 4200 Å. However, on some diodes a response was noted up to 5500 Å which indicates a level of about 2.0 eV. No information is available on what impurity would cause a trap at this level.

In summary, the multi-transition solar cell is quite attractive in that more than an order of magnitude increase in efficiency is apparently obtainable. A further plus feature for this type of operation is that the fabrication procedure is simple, being the same as for a single p-n junction device.

However, a large amount of effort would be needed to further investigate this process, including theoretical work to determine maximum trap density, effect of the traps on absorbtion characteristic etc. Experimental work would include doping crystals with various impurities and determining their energy level.

VI. CONCLUSIONS AND RECOMMENDATIONS

- SiC p-n junctions are operable as solar cells to 400°C although the power output is reduced at these temperatures. The structures will survive temperatures to 1000°C. The optimum power-temperature point is near 250°C.
- Solar cells can be fabricated from the largest crystals presently available (about 0.3 cm^2 area), thus simplifying fabrication of large area arrays.
- The work indicated that highly graded structures with junction depths near 15 microns are needed for the solar cell. Grown junction crystals, due to their lower sheet resistance, are preferred to diffused structures.
- Gridded top contacts are feasible using either brazed-on tungsten mesh or conductive epoxy. The use of gridded contacts increases the power output by a factor of two over dot contacts.
- The junction depth of the cells can be tailored to match the temperature and photon spectra.
- Cells connected in series and parallel behave as expected with no significant effects due to mis-matching. This would indicate a large area SiC solar cell array is feasible.
- Previous work has indicated SiC structures are about an order of magnitude more radiation resistant than silicon. Thus SiC solar cells should be usable in high radiation ambients.
- The multijunction solar cell and the multitransition cell, have been investigated. Although much work is needed, both of these structures would enhance the efficiency of the device.
- It is recommended that further work deal primarily with increasing the size of the SiC crystals together with improving their crystalline and electronic perfection. Grown junction crystals with a suitably graded junction should also be produced. Development of an anti-reflection coating should also be carried out as this could give up to 50% more power on any of the cells developed. In addition, the more complex structures should be studied and their fabrication demonstrated.

Successful completion of the above would provide a solar cell uniquely suited for high temperature-near sun missions.

VII. REFERENCES

(1) F. S. Johnson; J. Meteorology, 11 No. 6, 1954, 431.

(2) W. J. Choyke and L. Patrick; Silicon Carbide - A High Temperature Semiconductor, Pergamon Press, New York, 1960, pp. 306.

(3) D. R. Hamilton; Reference 2 pp. 43.

(4) R. B. Campbell and H. S. Berman, Material Res. Bull. 4, 1969, S-211 and references therein.

(5) H. C. Chang, L. F. Wallace and C. Z. LeMay; Reference 2, pp. 496.

(6) H. C. Chang et al; AL-TDR-630253; Final Report to Air Force Avionics Laboratory, Wright-Patterson Air Force Base, Ohio, 1963.

(7) Westinghouse Astronuclear Laboratory, unpublished data.

(8) We wish to thank Dr. Maurice Francombe of the Westinghouse Research Center for his assistance.

(9) We wish to thank Dr. W. J. Choyke of the Westinghouse Research Laboratories for calibrating standard detectors.

(10) H. K. Gunmel and F. M. Smits; PIC-SOL 209/2.1, Proc. of Solar Working Group Conf., Solar Power System Calib. and Testing, Vol. 2; February 1962.

(11) e.g. S. Friedlander et al; Final Report on Contract NAS2-3613. Ames Research Center.

(12) J. J. Capart; "Design of Solar Cells with Two Collecting Junction", ESROTN-3 (1966) also available as N68-16371.

(13) M. Wolf; Proc. IRE, 48 1960, pp. 1246.

(14) Contract AF 33(615)1189 with Wright-Patterson Air Force Base, Ohio.

(15) A. R. Verma, "Crystal Growth and Dislocation", Butterworth Scientific Publications Ltd. London, 1953.

(16) W. Shockley and W. T. Read, Jr., Phys. Rev., 8, 1952, 835.

(17) H. C. Chang et al; Final Report to Air Force Avionics Laboratory; AL TR-6-111; Wright-Patterson Air Force Base, Ohio 1966.

(18) R. B. Campbell and T. L. Chu, J. Electrochem. Soc. 113, 1966, 825.